Methyl and ethyl chloride synthesis in microreactors

Sabrina Andrea Schmidt

Laboratory of Industrial Chemistry and Reaction Engineering
Process Chemistry Centre
Department of Chemical Engineering
Åbo Akademi University
Turku/Åbo, 2014

Sabrina Andrea Schmidt

Born 1985 in Aachen, Germany

Diplom-Chemikerin 2010,
RWTH University Aachen, Germany

Methyl and ethyl chloride synthesis in microreactors

Sabrina Andrea Schmidt

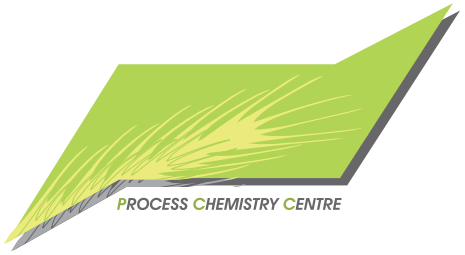

Laboratory of Industrial Chemistry and Reaction Engineering
Process Chemistry Centre
Department of Chemical Engineering
Åbo Akademi University
Turku/Åbo, Finland, 2014

Supervised by

Academy Professor Tapio O. Salmi
Laboratory of Industrial Chemistry and Reaction Engineering
Process Chemistry Centre
Åbo Akademi University
Turku/Åbo, Finland

and

Professor Dmitry Yu. Murzin
Laboratory of Industrial Chemistry and Reaction Engineering
Process Chemistry Centre
Åbo Akademi University
Turku/Åbo, Finland

Reviewers

Dr. José Rafael Hernández Carucci

Prof.Dr.ir. J.C. Schouten

Opponent

Prof.Dr.ir. J.C. Schouten

ISBN 978-952-12-3101-8

Painosalama Oy - Turku/Åbo, Finland 2014

PREFACE

The present work was carried out at the Laboratory of Industrial Chemistry and Reaction Engineering, Department of Chemical Engineering at Åbo Akademi University between September 2010 and August 2014. The research is part of the activities at Åbo Akademi Process Chemistry Centre (PCC). Financial support from the Academy of Finland is gratefully acknowledged. Furthermore the temporary financial support from the Graduate School of Chemical Engineering (GSCE) is gratefully acknowledged.

I would like to express my gratitude to Professor Tapio Salmi for giving me the opportunity to do this thesis at the Laboratory under his supervision. I am very grateful that Tapio Salmi, Dmitry Murzin and Narendra Kumar to share their wisdom with me and guided me for these four years. Special thanks go to Kari Eränen, who significantly contributed to this work by building the setup and keeping all equipment at Teknisk Kemi up and running. Furthermore I would like to thank Johan Wärnå and Nicola Gemo for their help in mathematical modeling and thank the visiting students Arne Reinssdorf, Quentin Balme and Zuzana Vajglova for their help and contributions to this work. I appreciate the work of Markus Peurla in many hours of TEM data acquisition and interpretation. For an inspiring research visit in Umeå University I would like to thank Natalia Bukhanko and J.-P. Mikkola.

It was a pleasure to work at this lab, a place with a great atmosphere and a melting pot of many different characters and cultures, thank you all!

Thanks my friends for sharing and caring: Victor, Gerson, Elena, Arne, Nora, Karch, Sonja, Jana, Uta, Claudi, Heidi, Tom, Kim, Matti, Pier, Jose, Odette, Andrea, Lotta, Steliana, Martina, Sevcan, Daniel, Frank, Phil, Antonina, Pascal.

Ich möchte auch meiner Familie (euch allen!) danken, die immer für mich da waren und sind.

Finalmente, Nicola, grazie.

Turku/Åbo, August 2014
Sabrina A. Schmidt

"People think that stories are shaped by people. In fact, it's the other way around."
— Terry Pratchett, Witches Abroad

ABSTRACT

Methyl and ethyl chloride synthesis in microreactors - from catalysis to product separation

Keywords: microreactor, kinetic modeling, internal diffusion modeling, chloromethane, chloroethane, catalyst coating, catalyst characterization, alumina, zeolites, zinc chloride.

Methyl chloride is an important chemical intermediate with a variety of applications. It is produced today in large units and shipped to the end-users. Most of the derived products are harmless, as silicones, butyl rubber and methyl cellulose. However, methyl chloride is highly toxic and flammable. On-site production in the required quantities is desirable to reduce the risks involved in transportation and storage.

Ethyl chloride is a smaller-scale chemical intermediate that is mainly used in the production of cellulose derivatives. Thus, the combination of on-site production of methyl and ethyl chloride is attractive for the cellulose processing industry, e.g. current and future biorefineries. Both alkyl chlorides can be produced by hydrochlorination of the corresponding alcohol, ethanol or methanol.

Microreactors are attractive for the on-site production as the reactions are very fast and involve toxic chemicals. In microreactors, the diffusion limitations can be suppressed and the process safety can be improved. The modular setup of microreactors is flexible to adjust the production capacity as needed.

Although methyl and ethyl chloride are important chemical intermediates, the literature available on potential catalysts and reaction kinetics is limited. Thus the thesis includes an extensive catalyst screening and characterization, along with kinetic studies and engineering the hydrochlorination process in microreactors.

A range of zeolite and alumina based catalysts, neat and impregnated with $ZnCl_2$, were screened for the methanol hydrochlorination. The influence of zinc loading, support, zinc precursor and pH was investigated. The catalysts were characterized with FTIR, TEM, XPS, nitrogen physisorption, XRD and EDX to identify the relationship between the catalyst characteristics and the activity and selectivity in the methyl chloride synthesis.

The acidic properties of the catalyst were strongly influenced upon the $ZnCl_2$ modification. In both cases, alumina and zeolite supports, zinc reacted to a certain amount with specific surface sites, which resulted in a decrease of strong and medium Brønsted and Lewis acid sites and the formation of zinc-based weak Lewis acid sites. The latter are highly active and selective in methanol hydrochlorination. Along with the molecular zinc sites, bulk zinc species are present on the support material.

Zinc modified zeolite catalysts exhibited the highest activity also at low temperatures (ca 200 °C), however, showing deactivation with time-on-stream. Zn/H-ZSM-5 zeolite catalysts had a higher stability than $ZnCl_2$

modified H-Beta and they could be regenerated by burning the coke in air at 400 °C. Neat alumina and zinc modified alumina catalysts were active and selective at 300 °C and higher temperatures. However, zeolite catalysts can be suitable for methyl chloride synthesis at lower temperatures, i.e. 200 °C.

Neat γ-alumina was found to be the most stable catalyst when coated in a microreactor channel and it was thus used as the catalyst for systematic kinetic studies in the microreactor. A binder-free and reproducible catalyst coating technique was developed. The uniformity, thickness and stability of the coatings were extensively characterized by SEM, confocal microscopy and EDX analysis. A stable coating could be obtained by thermally pretreating the microreactor platelets and ball milling the alumina to obtain a small particle size. Slurry aging and slow drying improved the coating uniformity.

Methyl chloride synthesis from methanol and hydrochloric acid was performed in an alumina-coated microreactor. Conversions from 4% to 83% were achieved in the investigated temperature range of 280-340 °C. This demonstrated that the reaction is fast enough to be successfully performed in a microreactor system. The performance of the microreactor was compared with a tubular fixed bed reactor. The results obtained with both reactors were comparable, but the microreactor allows a rapid catalytic screening with low consumption of chemicals. As a complete conversion of methanol could not be reached in a single microreactor, a second microreactor was coupled in series. A maximum conversion of 97.6 % and a selectivity of 98.8 % were reached at 340°C, which is close to the calculated values at a thermodynamic equilibrium.

A kinetic model based on kinetic experiments and thermodynamic calculations was developed. The model was based on a Langmuir Hinshelwood-type mechanism and a plug flow model for the microreactor. The influence of the reactant adsorption on the catalyst surface was investigated by performing transient experiments and comparing different kinetic models. The obtained activation energy for methyl chloride was ca. two fold higher than the previously published, indicating diffusion limitations in the previous studies. A detailed modeling of the diffusion in the porous catalyst layer revealed that severe diffusion limitations occur starting from catalyst coating thicknesses of 50 µm. At a catalyst coating thickness of ca 15 µm as in the microreactor, the conditions of intrinsic kinetics prevail.

Ethanol hydrochlorination was performed successfully in the microreactor system. The reaction temperature was 240-340°C. An almost complete conversion of ethanol was achieved at 340°C. The product distribution was broader than for methanol hydrochlorination. Ethylene, diethyl ether and acetaldehyde were detected as by-products, ethylene being the most dominant by-product. A kinetic model including a thorough thermodynamic analysis was developed and the influence of adsorbed HCl on the reaction rate of ethanol dehydration reactions was demonstrated.

The separation of methyl chloride using condensers was investigated. The proposed microreactor-condenser concept enables the production of methyl chloride with a high purity of 99%.

REFERAT

Syntes av metyl- och etylklorid i mikroreaktorer – från katalys till produktseparering

Nyckelord: Mikroreaktor, kinetisk modellering, modellering av intern diffusion, klormetan, kloretan, katalysatorns ytbeläggning, karakterisering av katalysatorn, zeolit, aluminiumoxid, zinkklorid

Metylklorid är en viktig kemisk mellanprodukt med många tillämpningar. I dagens läge produceras metylklorid i stora enheter och transporteras därefter till slutanvändare. Största delen av produkter som framställs med hjälp av metylklorid är oskadliga, såsom silikoner, butylgummi och metylcellulosa. Metylklorid själv är däremot ett ytterst giftigt och brandfarligt ämne. Produktion av metylklorid på ort och ställe, s.k. *on site* –produktion i önskade mängder är därför synnerligen önskvärd, eftersom riskerna med transport och lagring då kan minimeras.

Etylklorid är en kemisk mellanprodukt som numera framställs i mindre skala, eftersom den huvudsakligen används för preparering av cellulosaderivat. Därför är en kombination av *on site* –produktion av metyl- och etylklorid ett attraktivt alternativ för industrier som processar cellulosa, t.ex. dagens och framtida bioraffinaderier. Båda alkylkloriderna kan framställas via hydroklorering av den motsvarande alkoholen, d.v.s. etanol eller metanol.

Mikroreaktorer är attraktiva och avancerade tekniska alternativ för *on site* –produktion om reaktionerna är snabba och involverar giftiga kemikalier. I mikroreaktorer kan diffusionsmotstånden undertryckas och processäkerheten förbättras. Mikroreaktorer har en modulstruktur, vilket möjliggör en flexibel justering av produktionskapaciteten enligt behovet.

Även om metyl- och etylklorid är viktiga kemiska mellanprodukter, är den tillgängliga litteraturen om potentiella katalysatorer och reaktionernas kinetik ytterst begränsad. Därför ingår en omfattande kartläggning av katalysatorer, katalysatorkarakterisering samt kinetiska studier och teknologiutveckling av hydrokloreringsprocesser i mikroreaktorer.

En serie av zeolit- och aluminiumoxidbaserade katalysatorer, både rena och impregnerade med $ZnCl_2$ undersöktes i hydroklorering av metanol. Zinkmängdens, bärarmaterialets, zinkprekursorns och pH:s effekt på katalysatorns aktivitet och selektivitet undersöktes. Katalysatorerna karakteriserades med FTIR, TEM, XPS, kväveadsorption, XRD, och EDX för att kunna identifiera sambanden mellan katalysatorkarakteristiken och aktiviteten och selektiviteten i syntes av metylklorid.

Katalysatorns sura egenskaper var starkt påverkade av modifieringen med $ZnCl_2$. I båda fallen, d.v.s. för aluminiumoxid- och zeolitbärare, reagerade zink i viss mån med specifika säten på katalysatorytan, vilket resulterade i en sänkning av starka och medelstarka Brönsted- och Lewissura säten samt en ökning av svaga Lewissura säten. De svaga Lewissura sätena är högaktiva och selektiva i hydroklorering av metanol. I bärarmaterialet finns utom molekylära zinkspecies även zink i bulkfasen.

Zinkmodifierade zeolitkatalysatorer uppvisade den högsta aktiviteten också vid låga temperaturer (ca 200°C), men de deaktiverades under reaktionens gång. Zn/H-ZSM-5 zeolitkatalysatorer hade en bättre stabilitet än $ZnCl_2$-modifierad betakatalysator och de kunde regenereras genom att bränna upp koksen i luft vid 400°C. Ren aluminiumoxid och zinkmodifierade aluminiumoxidkatalysatorer var aktiva och selektiva vid 300°C och högre temperaturer. Zeolitkatalysatorer kan däremot vara lämpliga för metylkloridsyntes vid lägre temperaturer, d.v.s. vid 200°C.

Ren gamma-aluminiumoxid visade sig vara den mest stabila katalysatorn som en beläggning i mikroreaktorkanaler och därför användes den som katalysator för systematiska kinetiska studier i mikroreaktorsystemet. En beläggningsteknologi där inga bindemedel ingår utvecklades. Beläggningens jämnhet, tjocklek och stabilitet karakteriserades grundligt med svepelektronmikroskopi, konfokalmikroskopi och EDX. En stabil beläggning erhölls genom att termiskt förbehandla mikroreaktorelementen och finmala aluminiumoxid för att uppnå en tillräckligt liten partikelstorlek. Genom att låta dispersionenåldras och torkas långsamt förbättrades katalysatorns jämnhet.

Metylkloridsyntes utgående från metanol och klorväte genomfördes i en aluminiumoxidbelagd mikroreaktor. Omsåttningsgrader 4 till 83% erhölls inom det undersökta temperaturintervallet 280-340°C. Detta demonstrerade att reaktionen är tillräckligt snabb för att kunna genomföras i ett mikroreaktorsystem. Mikroreaktorns prestanda jämfördes med prestandan av en konventionell packad bäddreaktor. Resultaten från båda reaktorerna var jämförbara, men genom att utnyttja en mikroreaktor kan en snabb kartläggning av olika katalysatorer göras med en låg konsumtion av kemikalier. Den maximala omsättningsgraden av metanol var 97,6% och metylkloridselektiviteten var 98,8% vid 340°C, vilket närmar sig den estimerade termodynamiska jämvikten.

En matematisk modell baserad på kinetiska experiment och termodynamiska beräkningar utvecklades. Modellen baserade sig på en Langmuir-Hinshelwoodmekanism och en kolvströmningsmodell för mikroreaktorn. Reaktantadsorptionens effekt undersöktes genom tidsberoende transienta experiment och en jämförelse av konkurrerande kinetiska modeller gjordes. Den estimerade aktiveringsenergin för metylklorid var ca dubbelt så stor som tidigare publicerade värden, vilket indikerar att diffusionsbegränsningar hade påverkat de tidigare publicerade resultaten. En detaljerad modellering av simultana reaktions- och diffusionsfenomen avslöjade att allvarliga diffusionsbegränsningar förekommer t.o.m. för katalysatorskikt med en tjocklek på 50 mikrometer. I mikroreaktorer är katalysatortjockleken typiskt ca 15 mikrometer, vilket innebär att betingelserna för en verklig diffusionsfri reaktionskinetik blir uppfyllda.

Hydroklorering av etanol genomfördes framgångsrikt i en mikroreaktor med aluminiumoxid som katalysatormaterial. Reaktionstemperaturen var 240-340°C. En nästan fullständig omsättning av etanol uppnåddes vid 340°C. En bredare produktfördelning uppnåddes jämfört med hydroklorering av metanol. Som reaktionsprodukter förekom bl.a. eten, dietyleter och acetaldehyd. Den huvudsakliga biprodukten var eten. En kinetisk modell innefattande en grundlig termodynamisk analys utvecklades

och inverkan av adsorberat klorväte på reaktionshastigheten för etanolhydreringsreaktionerna påvisades.

Separering av metylklorid ur reaktionsblandningen genom kontinuerlig kondensation undersöktes. Det föreslagna mikroreaktor-kondensorkonceptet möjliggör produktion av metylklorid med en hög renhet, ca 99%.

Zusammenfassung

Methyl- und Ethylchlorid Synthese in Mikroreaktoren

Schlüsselwörter: Mikroreaktor, kinetische Modellierung, Modellierung interner Diffusion, Chlormethan, Chlorethan, Katalysatorbeschichtung, Katalysatorcharakterisierung, Zeolithe, Aluminiumoxid, Zinkchlorid

Methylchlorid ist ein wichtiges Zwischenprodukt der chemischen Wertschöpfungskette mit einer Vielzahl von Anwendungen. Es wird in großen Anlagen produziert und zur verbrauchenden Industrie transportiert. Während Methylchlorid hochgiftig und leichtentzündlich ist, sind die meisten der mit Methylchlorid synthetisierten Produkte wie zum Beispiel Silikone, Butylkautschuk und Methylcellulose harmlos. Eine Produktion direkt beim Endverbraucher (on-site) in den gewünschten Mengen wäre vorteilhaft um Risiken verbunden mit Transport und Lagerung zu vermeiden.

Ethylchlorid ist ein chemisches Zwischenprodukt mit geringerem Umsatz und wird hauptsächlich bei der Produktion von Zellulosederivaten verwendet. Die Kombination der on-site Ethyl- und Methylchlorid Produktion ist aus oben genannten Gründen attraktiv für die Zellulose-verarbeitende Industrie, wie zum Beispiel einer Bioraffinierie. Beide Alkylchloride können durch Hydrochlorierung des entsprechenden Alkohols hergestellt werden.

Mikroreaktoren sind attraktiv für die on-site Produktion von Methyl- und Ethylchlorid, da die Reaktionen sehr schnell sind und giftige Stoffe involvieren. Diffusionslimitierungen können in Mikroreaktoren unterdrückt und die Sicherheit des Prozesses verbessert werden. Außerdem sind Mikroreaktoranlagen modular aufgebaut und sind deshalb flexibel und können der gewünschten Produktionskapazität angepasst werden.

Obwohl Methyl- und Ethylchlorid ein wichtiges Zwischenprodukt darstellen, ist die verfügbare Literatur über Katalysatoren und Kinetik sehr begrenzt. Deswegen enthält diese Arbeit neben Kinetischen Studien und der technischen Umsetzung der Hydrochlorierungsreaktionen auch eine umfangreiche Studie möglicher Katalysatoren mit detaillierter Katalysatorcharakterisierung.

Eine Reihe Zeolith- und Aluminiumoxidbasierter Katalysatoren, rein und imprägniert mit Zinkchlorid, wurden für die Methanol Hydrochlorierung getestet. Der Einfluss von Zinkgehalt, Katalysatorträger, Zinkvorstufe und pH wurden untersucht. Die Katalysatoren wurden mit Hilfe von FTIR-Spektroskopie, Transmissionselektronenmikroskopie, Röntgenphotoelektronenspektroskopie, Stickstoffadsorption, Röntgenstrukturanalyse, und Energiedispersiver Röntgenspektroskopie charakterisiert um den Zusammenhang zwischen den Katalysatoreigenschaften und der Aktivität und Selektivität in der Methylchloridsynthese zu finden.

Die sauren Eigenschaften der Katalysatoren wurden stark von der Imprägnation mit Zinkchlorid beeinflusst. Sowohl bei Zeolithen als auch bei Aluminiumoxid reagierte Zink mit einer bestimmten Menge von aktiven Oberflächengruppen der Katalysatorträger. Dies führte zu einer Abnahme der starken und mittelstarken Brønsted-und Lewis-sauren Gruppen und

der Bildung von schwachen zinkbasierten Lewis-sauren Gruppen. Diese schwachen Lewis-sauren Gruppen sind hoch aktiv und selektiv in der Methanol Hydrochlorierung. Neben den molekularen Zink-Gruppen sind auch makroskopische Zinkverbindungen auf der Katalysatoroberfläche vorhanden.

Zinkmodifizierte Zeolithe waren am aktivsten, und das auch bei niedrigen Temperaturen (200 °C), deaktivierten aber mit der Reaktionszeit. Zn/H-ZSM-5 Katalysatoren waren stabiler als Zn/H-Beta Katalysatoren und konnten durch Erhitzen auf 400 °C in Luft wieder regeneriert werden. Aluminiumoxid, rein und Zinkmodifiziert war erst bei Temperaturen von 300 °C oder höher vergleichbar aktiv und selektiv. Trotz der Deaktivierung können Zeolithbasierte Katalysatoren für die Methylchloridsynthese bei niedrigeren Temperaturen (z.B. 200 °C) geeignet sein.

Reines gamma-Aluminiumoxid war der stabilste Katalysator im Fall einer Beschichtung von Mikroreaktorkanälen und wurde deshalb für systematische Studien der Reaktionskinetik der Hydrochloriererungsreaktionen verwendet. Eine Bindemittelfreie und reproduzierbare Katalysator-Beschichtungsmethode wurde entwickelt. Die Uniformität, Stabilität und Dicke der Katalysatorschichten wurden mit Hilfe von Rasterelektronenmikroskopie, konfokaler Mikroskopie und Energiedispersiver Röntgenspektroskopie genau analysiert. Eine stabile Beschichtung der Kanäle mit Katalysator konnte erhalten werden, indem das Mirkroreaktorplättchen thermal vorbehandelt wurde und das Katalysatorpulver mit einer Kugelmühle fein zermahlen wurde. Eine kontrollierte Alterung der Katalysatordispersion und ein langsames Trocknen der beschichteten Plättchen verbesserte die Uniformität der Beschichtung.

Die Methylchloridsynthese wurde in einem einzelnen Aluminiumoxid-beschichteten Mikroreaktor durchgeführt. Umsätze von 4-83% wurden im untersuchten Temperaturbereich von 280-340 °C erreicht. So wurde gezeigt, dass die Reaktion ausreichend schnell ist, um in Mikroreaktoren durchgeführt zu werden. Der erreichte Durchsatz wurde mit dem eines Festbettreaktors (Ø 1 cm) verglichen. Die Ergebnisse beider Reaktoren waren vergleichbar, aber der Mikroreaktor erlaubt ein schnelles Durchführen von katalytischen Testreihen mit geringem Verbrauch an Chemikalien. Da ein vollständiger Umsatz von Methanol in einem einzelnen Mikroreaktor nicht erreicht werden konnte, wurde ein zweiter seriell gekoppelt. So wurde ein maximaler Umsatz von 97.6% und eine Selektivität von 98.8% bei einer Temperatur von 340 °C erreicht, was nahe dem berechneten thermodynamischen Gleichgewicht liegt.

Ein kinetisches Modell auf Grundlage von kinetischen Messungen und thermodynamischen Berechnungen wurde entwickelt. Das Modell basiert auf dem Langmuir-Hinshelwood Mechanismus und dem Pfropfenströmungsmodell für den Mikroreaktor. Der Einfluss von Adsorptionsprozessen auf der Katalysatoroberfläche wurde mit Hilfe von transienten Experimenten und dem Vergleich von verschiedenen kinetischen Modellen ermittelt. Die so erhaltenen Aktivierungsenergien und präexponentiellen Faktoren waren etwa doppelt so hoch wie die zuvor publizierten, was auf Diffusionslimitierungen in diesen Studien hinweist. Eine detailliertes Modell der Diffusionsprozesse in einer porösen Katalysatorschicht zeigte, dass starke Diffusionslimitierungen vorliegen, wenn die Katalysatorschicht dicker als 50 µm ist. Bei einer Schichtdicke von

15 µm, wie im verwendeten Mikroreaktor, herrschen intrinsische Reaktionsgeschwindigkeiten.

Ethanol Hydrochlorierung wurde erfolgreich in zwei seriell gekoppelten Reaktoren durchgeführt. Die Reaktionstemperatur war zwischen 240 und 340 °C. Ein nahezu kompletter Ethanolumsatz konnte bei 340 °C erreicht werden. Im Fall der Ethanol Hydrochlorierung gab es mehr Nebenprodukte als bei der Methanol Hydrochlorierung. Ethen, Diethylether und Acetaldehyd wurden gebildet, wobei Ethen das wichtigste Nebenprodukt war. Ein kinetisches Modell inklusive einer thermodynamischen Analyse wurde entwickelt und der Einfluss der auf der Katalysatoroberfläche adsorbierten Salzsäure auf die Dehydrierungsreaktionen des Ethanols wurde demonstriert.

Die Trennung des Methylchlorids mit Hilfe von Kondensatoren (Laborkühlern) wurde untersucht. Das vorgeschlagene Mikroreaktor-Kondensator-Konzept ermöglicht die Produktion mit einer Reinheit von 99%.

LIST OF PUBLICATIONS

I. S.A. Schmidt, N. Kumar, B. Zhang, K. Eränen, D. Murzin, T. Salmi, Preparation and characterization of alumina-based microreactors for application of methyl chloride synthesis Ind Eng Chem. Res. 2012, 51, 4545-4555.

II. S.A. Schmidt, N. Kumar, A., Shchukarev, K. Eränen, J.-P. Mikkola, D. Murzin, T. Salmi Preparation and characterization of neat and $ZnCl_2$ modified zeolites and alumina for methyl chloride synthesis Appl. Catal. A. 2013, 468, 120-134.

III. S. A. Schmidt, M. Peurla, N. Kumar, K. Eränen, D. Yu. Murzin, T. Salmi, Preparation of selective $ZnCl_2$/alumina catalysts for methyl chloride synthesis: Influence of pH, precursor and zinc loading (submitted).

IV. S. A. Schmidt, N. Kumar, A. Reinsdorf, K. Eränen, J. Wärnå, D., Murzin, T., Salmi, Methyl chloride synthesis on Al_2O_3 in a microstructured reactor – thermodynamics, kinetics and mass transfer, Chem. Eng. Sci 2013, 95, 232-245.

V. S. A. Schmidt, Q. Balme, N. Gemo, N. Kumar, K. Eränen, D. Yu. Murzin, T. Salmi, Kinetics of ethanol hydrochlorination over γ-Al_2O_3 in a microstructured reactor (submitted).

VI. S. A. Schmidt, Z. Vajglova, K. Eränen, D. Murzin, T. Salmi, Microreactor technology for on-site production of methyl chloride. Green Process. Synth. 2014, Advance online publication, DOI: 10.1515/gps-2014-0039.

OTHER PUBLICATIONS RELATED TO THE TOPIC

1. S. Schmidt, N. Kumar, B. Zhang, K. Eränen, J. E. Eriksson, T. Salmi, D. Yu. Murzin, Preparation and characterization of alumina-based microreactors for application in methyl chloride synthesis. 12th International conference on microreaction technology, 20-22 February 2012, Lyon, France (Oral presentation).
2. S. A. Schmidt, N. Kumar, K. Eränen, D. Yu. Murzin, T. Salmi, Novel catalysts for methyl chloride synthesis – Zn modified H-Beta zeolites. The 15th Nordic Symposium on Catalysis. 10-12 June 2012, Mariehamn, Åland. (Poster presentation).
3. S. Schmidt, N. Kumar, A. Reinsdorf, R. Lange, K. Eränen, D. Y. Murzin, T. Salmi, Kinetics of methanol hydrochlorination in a microreactor. 20th International Congress of Chemical and Process Engineering. 25-29 August 2012, Prague, Czech Republic (Oral presentation).
4. S. A. Schmidt, N. Kumar, K. Eränen, D. Yu. Murzin, T. Salmi, Microreactor technology in the preparation of chemical intermediates: synthesis of methyl chloride. 9th European Congress of Chemical Engineering, 21-25 April 2013, the Hague, The Netherlands (Poster presentation).
5. S. A. Schmidt, N. Kumar, K. Eränen, D. Yu. Murzin, T. Salmi, Methyl chloride synthesis over ZnCl2 modified zeolites and alumina -Relation between acidity, activity and selectivity. 7th International Symposium on Acid-Base Catalysis, 12-15 May 2013, Tokyo, Japan (Oral presentation).
6. S. A. Schmidt, Z. Vajglova, K. Eränen, D. Y. Murzin, T. Salmi, Microreactor technology for on-site production of methyl chloride. 4th International Congress on Green Process Engineering, 7-10 April 2014 – Sevilla, Spain (Keynote lecture).
7. S. A. Schmidt, J. Wärnå, Z. Vajglova, N. Kumar, K. Eränen, D. Yu. Murzin, T. Salmi, Methyl chloride synthesis in a microreactor-Development of a small-scale production unit. 13th International conference on microreaction technology, 23-25 June 2014, Budapest, Hungary (Oral presentation).

Table of Content

1 Introduction

1.1 Methyl chloride and ethyl chloride

1.1.1 Methyl chloride

Methyl chloride or chloromethane (MeCl) is a large-scale chemical intermediate with an annual production of ca. 10^6 t and a growing market [1,2]. It is used as a general methylation agent, for example in the industrial production of methyl cellulose, silicones and rubber. Moreover, it is a highly toxic and flammable component (Figure 1).

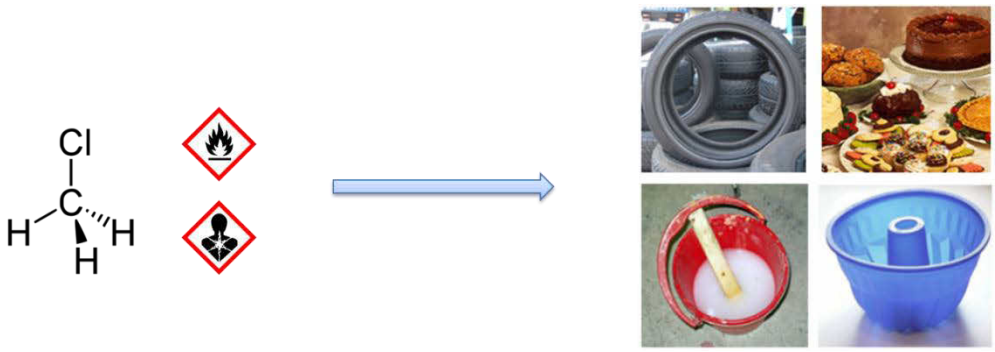

Figure 1: Methyl chloride and its end-products. [3]

Methyl chloride can be produced by two methods: hydrochlorination of methanol with HCl or chlorination of methane with molecular chlorine. The latter method leads to a product mixture of chloromethanes with a varying degree of chlorination and requires higher temperatures (up to 550 °C) [1]. Due to the higher selectivity, methanol hydrochlorination is the favored process for methyl chloride production. The reaction scheme is shown below:

$$CH_3OH + HCl \leftrightarrow CH_3Cl + H_2O \quad (I)$$

$$2\ CH_3OH \leftrightarrow (CH_3)_2O + H_2O \quad (II)$$

$$(CH_3)_2O + HCl \leftrightarrow CH_3Cl + CH_3OH \quad (III)$$

Alongside with methyl chloride, dimethyl ether (DME) is formed as a side product (II). DME can react further with HCl to form methanol (MeOH) and MeCl (III).

1.1.2 Ethyl chloride

Ethyl chloride (EtCl) or chloroethane is a chemical intermediate that is used as a general ethylation agent and local anesthetic. In the past ethyl chloride was produced in large amounts for the production of the fuel additive tetraethyllead (TEL) [1,4]. However, the situation has changed, since TEL is nowadays banned throughout the world and ethyl chloride production is sharply decreasing [1,4]. In the future, the main use of this chemical might be cellulose ethylation. Ethyl cellulose is a versatile chemical that can be used amongst others as thickener, emulsifier, filmogen and flocculent [5]. In the past, the main production route was ethanol hydrochlorination, but due to the high price of ethanol, the main production route today is ethylene hydrochlorination. However, with a shift to renewable resources, ethanol can become an attractive raw material and its hydrochlorination the most attractive and sustainable route for the ethyl chloride production.

The reaction scheme for the ethanol hydrochlorination is more complex than in the case of methanol. Several side-products are formed and possible side reactions can take place. A possible reaction scheme is shown below. The main reaction is the formation of ethyl chloride from ethanol and HCl (I). Ethanol dehydration to diethyl ether (II) and ethylene (III) takes place, too. Ethanol is furthermore dehydrogenated to acetaldehyde (V) in small amounts. Additionally, it is possible that diethyl ether (VI) reacts with HCl to form ethyl chloride and a disproportionation of diethyl ether to ethylene and ethanol can take place [6,7] (IV). At elevated temperatures ethyl chloride can decompose to ethylene and HCl (VII). A range of other by-products such as ethane, butylenes, methane and propylenes [8] can be formed as well although in insignificant amounts. The reaction scheme is shown below.

$$EtOH + HCl \rightarrow EtCl + H2O \quad (I)$$
$$2\ EtOH \rightarrow DEE + H2O \quad (II)$$
$$EtOH \rightarrow C_2H_4 + H2O \quad (III)$$
$$DEE \rightarrow C_2H_4 + EtOH \quad (IV)$$
$$EtOH \rightarrow CH_3CHO + H_2 \quad (V)$$
$$DEE + HCl \rightarrow EtCl + EtOH \quad (VI)$$
$$EtCl \rightarrow C_2H_4 + HCl \quad (VII)$$

1.2 Catalysts for methyl and ethyl chloride synthesis

Lewis acid sites (LAS) are needed to catalyze these reactions. Alumina, either neat or modified with zinc chloride is used industrially for methanol hydrochlorination [9] and can be used as well for ethanol hydrochlorination. Other supports have also been investigated and it has been shown that alumina, aluminum silicate and silica supported catalysts are more active than carbon supported catalysts [10]. Several metal chlorides supported on alumina have been screened for methyl chloride synthesis [11] as they increases the activity and selectivity towards methyl chloride. Zinc chloride was the most efficient modifier [10].

In an early work the influence of zinc modification on the heat of adsorption of HCl and methanol on alumina and $ZnCl_2$/alumina was studied to characterize the catalyst [10]. Three different adsorption sites on $ZnCl_2$ modified alumina were suggested: alumina surface sites, $ZnCl_2$ monolayer sites and bulk $ZnCl_2$ sites (≥ 2 layers). In the case of methanol adsorption an optimum zinc content was found, i.e. a zinc loading at which the heat of adsorption for methanol was maximal. This was the case for the catalyst with the highest number of $ZnCl_2$ monolayer sites (60 wt%). Although the heat of adsorption was maximal at a $ZnCl_2$ loading of 60 wt% the surface area decreased from 180 to 79 m^2/g. At even higher $ZnCl_2$ loadings, the heat of adsorption decreased again due to the appearance of bulk $ZnCl_2$ sites. Thus, a too high $ZnCl_2$ loading is not desirable, due to the surface area decrease and formation of $ZnCl_2$ sites less suitable for the methanol adsorption. On the contrary, the heat of adsorption of HCl was only weakly dependent on the $ZnCl_2$ loading.

In recent years $ZnCl_2$/alumina catalysts have gained an increased interest, since they were used as catalyst for other kinds of reactions e.g. olefin metathesis in combination with CH_3ReO_3 [12-14] and hydrochlorination of ethene [15]. A deeper characterization of zinc modified alumina catalysts has been carried out to identify active sites and understand the physico-chemical and catalytic properties. Different active species have been proposed, such as amorphous zinc chloride [15] and a molecular zinc species on the alumina surface [12]. A common observation is that upon zinc modification of alumina, terminal hydroxyl groups are eliminated which suggests that zinc reacts directly with the alumina surface [12-14]. This is also supported by the observation of a chlorine-to-zinc ratio lower than two when the catalyst was calcined at higher temperatures [12]. As the active zinc species is still under discussion and no information is available on the Lewis acidic properties of the zinc-modified catalysts, a deeper characterization of zinc modified alumina becomes necessary.

Besides alumina, also zeolites are attractive supports for zinc chloride and potential catalysts for methanol and ethanol hydrochlorination. Furthermore, zinc modified zeolites can also be used to catalyze other reactions, e.g. aromatization of propane [16], Heck reaction [17], dehydrogenation of ethane [18], dehydrogenation and isomerization of butane [19] and other hydrocarbons [20]. More detailed catalyst characterization has been performed for $ZnCl_2$ modified zeolites, but due to a more complex nature of zeolites, the state of zinc in the catalyst is still under debate. Different kinds of zinc species formed by ion exchange have

been suggested [21-24] alongside with reaction of zinc with extra-framework aluminum [25] and the formation of extra crystalline ZnO at higher zinc loadings [16,26].

The following main conclusions have been drawn for the interaction of zinc ions with zeolites:

i. Mainly strong Brønsted acid sites (BAS) are involved in ion exchange, while weak BAS are retained [27].

ii. In the case of divalent ions, such as Zn^{2+}, vicinal BAS are preferred for ion exchange, isolated BAS remain [16,28].

iii. In the case of Zn/Al < 0.26, zinc species are isolated; at higher loading the formation of ZnO nanocrystals is proposed [16,27,28]. Reaction with extra-framework aluminum is possible as well.

An overview of probable Lewis acid sites according to Biscardi et al. [16] and Lercher et al. [28] is shown in Figure 2.

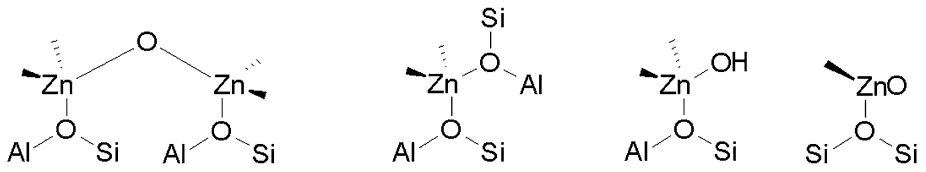

Figure 2: Possible species of zinc on zeolites according to Biscardi et al. [16] and Lercher et al. [28].

1.2.1 Kinetics of methanol and ethanol hydrochlorination

1.2.1.1 Methyl chloride

A few publications deal with the kinetics of this reaction over alumina catalysts [9,11,29-32]. The studies mainly deal with neat alumina catalysts and report the methyl chloride formation, reaction (I), to be dominant, while reactions (II) and (III), which consider the reactions of dimethyl ether are regarded as negligible. It has however been demonstrated that dimethyl ether is present in the reaction mixture in a considerable amount at low methanol conversions [9]. With an increased reaction time, however, the dimethyl ether concentration decays due to reaction (III).

The reactions are very rapid and slightly exothermic, making microreactors an ideal tool for kinetic studies of methanol hydrochlorination within the regime of intrinsic kinetics.

1.2.1.2 Ethyl chloride

So far only one investigation on ethanol hydrochlorination has been published [33]. Neat and $ZnCl_2$ modified aluminas have been tested and activation energies for the hydrochlorination reaction of ethanol have been reported. However, the study focused more on the catalyst development and screening of the reaction conditions and the kinetic model does not account for the formation of by-products such as ethylene and diethyl ether. As in the case of methanol, ethanol hydrochlorination is a rapid reaction, making a kinetic study in microreactors very attractive.

While ethanol hydrochlorination is barely investigated, ethanol dehydration reactions on alumina are intensively studied and the results can be used to clarify the reaction mechanisms in ethanol hydrochlorination. In early studies by Knözinger and Köhne diethyl ether formation is reported to be preferred at lower temperatures but ethylene at higher temperatures [6,7]. Acetaldehyde formation is not favorable on alumina, but is produced in smaller amounts [7,34]. However, the role of water and ethanol adsorption on the reaction rates of ether and ethylene production is still under discussion. Water is thought to compete with ethanol for the adsorption sites on alumina [35,36]. The role of water as an inhibitor of ethanol dehydration reactions is discussed as well as the kinetics of ethylene and diethyl ether formation. According to DeWilde et al. [35] the activation energies of both reactions are similar but the selectivity to ether or ethylene depends on the surface coverage of alumina by ethanol. In one study, ethanol adsorption is not taken into account [8].

1.3 Microreactor technology

Microreactors are reactor structures in which at least one inner dimension is in the sub-millimeter range [37]. With the decrease of the specific length scale in a reactor many advantages arise, which makes microreactor technology a promising field of research and development [38-40]. The most important difference between a microstructured and a conventional reactor is the dramatic increase of the surface-to-volume ratio in a microreactor. While it is 100-1000 m^2/m^3 in conventional reactors, the ratio goes up to 10,000 to 50,000 m^2/m^3 in microreactors [41]. This is especially beneficial for heterogeneous catalyzed reactions, where the catalyst is coated on the microreactor channels as it is the case in this work. Furthermore, a very good heat transfer (~25.000 W/m^2) is guaranteed [41]. Diffusion distances are short, therefore that internal and external diffusion limitations are suppressed. Efficient mass transfer is facilitated and local mixing is very rapid [42]. Due to a small inner volume, the residence time can be very short. In the narrow microreactor channels laminar flow often prevails. The parabolic velocity profile of laminar flow can

broaden the residence time distribution. However, short radial diffusion times [43] and an optimized channel geometry can lead to very narrow residence time distributions [44]. This is beneficial for processes involving consecutive reactions which impair the product selectivity. The decrease of the inner volume also provides a lower material holdup and inherent safety due to the explosion suppression [38]. The use of microreactors is especially attractive in case of fine chemical synthesis as well as fast and hazardous reactions.

The main drawbacks for the industrial application of microreactors are the high material cost and a low production capacity.

1.4 Research motivation

The motivation of this work is to demonstrate the feasibility of microreactors for the on-site production of methyl and ethyl chloride. As methyl and ethyl chloride are highly toxic, on-site production decreases the safety risks due to transportation and storage. The process safety is increased due to a low chemical holdup of microreactors. Furthermore, the reactions are very fast, so that the catalyst and space-efficiency of the process are increased when microstructured reactors are used.

Furthermore, an on-site integration of ethyl and methyl chloride synthesis into a biorefinery is very attractive. Ethanol, methanol and cellulose can be produced on site and further converted to (m)ethyl chloride and (m)ethyl cellulose. Both cellulose derivatives are versatile products that can be valuable end-products of an integrated biorefinery.

This work aims to give an adequate understanding of several crucial aspects of reaction engineering and reactor technology applied to microreactors. The research effort includes catalyst development and characterization, catalyst coating technology, detailed kinetic studies and product separation.

2 Experimental

2.1 Preparation of catalysts and catalyst coating

2.1.1 Catalyst preparation

2.1.1.1 Pure alumina

A commercial γ-alumina powder (UOP Versal VGL-25) was ball-milled and sieved to obtain a particle size smaller than 32 µm. The d_{50} and d_{90} of the catalyst powder were determined from SEM pictures to be d_{50} = 5 µm and d_{90} = 11 µm.

2.1.1.2 Zinc modified alumina and zeolites

As catalysts and supports for $ZnCl_2$ (Fluka, ≥ 98%) the following materials were applied: H-Beta 25 (from NH_4-Beta 25, Zeolyst, CP814E), H-Beta 150 (Zeolyst, CP811E) H-Beta 300 (Zeolyst, CP811C-300), H-ZSM580 (from NH_4-ZSM580, Zeolyst, CBV8014), H-ZSM5280 (from NH_4-ZSM5 280, Zeolyst, CBV2814) and γ-alumina (UOP Versal VGL-25). H-Beta 150 and alumina were used as received. The NH_4-zeolites were transformed to their proton forms by calcination at 450 °C for three hours. H-Beta 300 was calcined as well to remove traces of remaining template used for its preparation.

The zinc chloride modified catalysts were prepared by wet impregnation as follows: 4 g of ball milled and sieved support (<32µm) were added to a solution of the desired amount of $ZnCl_2$ in 200 mL distilled water. The loading in wt% refers to the amount of zinc ions on the alumina. The initial pH values of the prepared solutions are listed in Table 1. The solution was rotated for 24 h at 65 °C, and subsequently, the water was evaporated at 70-80 °C under vacuum. The catalyst was calcined for 3 h at 400 °C, applying a heating rate of 3 °C/ min. Prior to heating to 400 °C, the catalysts were kept for 40 min at 200 °C.

Table 1: pH of the support/$ZnCl_2$ dispersion for impregnation

Zeolite catalysts	pH	Alumina catalysts	pH
$ZnCl_2$/H-Beta25	3.5	Alumina 2.4 wt% Zn ($ZnCl_2$)	5.6
$ZnCl_2$/H-Beta150	3.8	Alumina 4.5 wt% Zn ($ZnCl_2$)	5.6
$ZnCl_2$/H-Beta300	5.5	Alumina 4.5 wt% Zn ($ZnCl_2$)	4.0
$ZnCl_2$/H-ZSM523	3.3	Alumina 4.5 wt% Zn ($ZnCl_2$)	8.5
$ZnCl_2$/H-ZSM5 80	3.8	Alumina 4.5 wt% Zn ($ZnCl_2$)	10.6
$ZnCl_2$/H-ZSM5 280	5.5	Alumina 4.5 wt% Zn ($Zn(NO_3)_2$)	6.0
		Alumina 8 wt% Zn ($ZnCl_2$)	5.7
		Alumina 14 wt% Zn ($ZnCl_2$)	5.6
		Alumina 19 wt% Zn ($ZnCl_2$)	5.4
		Alumina 22 wt% Zn ($ZnCl_2$)	5.4
		Alumina 25 wt% Zn ($ZnCl_2$)	5.3

2.1.2 Catalyst coating of the microreactor platelets

2.1.2.1 Pretreatment of microreactor platelets

In order to remove impurities, the catalyst platelets were cleaned with soap and distilled water, subsequently with acetone and finally flushed with distilled water. The clean platelets were then pretreated to create a sufficient surface roughness for a better catalyst adhesion. Two different methods were applied. In thermal pretreatment, the platelets were calcined in air at 648 K for 40 min and 1023 K for 3 h, using a heating rate of 3 K/min. In the acid pretreatment, the platelets were etched for 40 min in a 12 wt% hydrochloric at 353 K. The pretreated surfaces of the platelets were characterized by confocal white light microscopy to determine the surface roughness and by energy-dispersive X-ray microanalysis to determine the surface elemental composition.

2.1.2.2 Slurry preparation and catalyst coating

The alumina coating was introduced by a slurry deposition method. The slurry was prepared by adding water and for some slurries a colloidal silica binder (Ludox AS-30, Aldrich). The particle size of the silica was determined by light scattering (Malvern Zetasizer) and found to be 7-13 nm. The addition of the binder increased the pH of the slurry to ~8.8, and the pH of the binderless slurry was set to 8.8 by addition of an ammonium hydroxide solution. To keep the overall solid content fixed, binderless slurry contained 14 wt% alumina and the slurry with binder had 10 wt% alumina and 4 wt% binder (colloidal silica). The slurry was stirred for four hours at

323 K and two days at ambient temperature. Only slurries not older than one day were used for coating, as hydrolysis of alumina in water is not negligible, which might change the coating characteristics [45].

The slurry was deposited on the platelets with the aid of a Finnpipette 0.5-10 µL. The amount of slurry dosed per platelet corresponded to its channel volume of 3 µL. As not every batch of the microreactor platelets had exactly the same depth, the volume of the slurry added could vary by ±0.3 µL. The platelets were dried in a fridge to allow a slow drying of the slurry. The catalyst not present in the channels but on the platelet surface was removed. Finally the platelets were calcined in air at 548 K for 40 min and 823 K for 3 h, applying a heating rate of 3 K/min.

The mass of slurry was determined by weighing the 10 catalyst platelets before and after the coating. The amount of catalyst on ten platelets was 3 to 4 mg, depending on the batch prepared and the slurry dosed. The catalyst coating thickness for the kinetic experiments was 15 ± 3 µm for methyl chloride and16 ± 4 µm for ethyl chloride.

2.2 Characterization of catalyst and catalyst coating

2.2.1 Catalyst powder characterization

2.2.1.1 Scanning electron microscopy (SEM) and energy dispersive X-ray analysis (EDX)

The elemental composition of the catalysts was determined by energy-dispersive X-ray micro analysis (EDX) (Zeiss Leo Gemini 1530). The catalysts used for the EDX analysis were pressed to wafers, as for the FTIR measurements. Due to the high density of the wafers, the quantification was more precise and charging of the zeolite samples during the measurement was reduced.

2.2.1.2 Nitrogen physisorption

For the surface area measurements a sorptometer (1900, Carlo Erba Instruments) was used. The samples were outgassed for three hours at 423 K prior to the measurement of the surface area. The surface area of alumina was calculated using the B.E.T method, while for zeolitic materials the Dubinin method was used for the surface area calculations. The Dollimore/Heal model was used to calculate the pore size.

2.2.1.3 Fourier transform infrared spectroscopy (FTIR)

The amount of Lewis and Brønsted acid sites on the catalysts was measured by Fourier transform infrared spectroscopy (FTIR) using pyridine

as the probe molecule (ATI Mattson Infinity Series). The catalyst was pressed to a wafer and placed in the measurement cell. Prior to the pyridine adsorption, the sample was outgassed under vacuum for one hour at 450 °C. Pyridine was adsorbed for 30-90 min at 100 °C and spectra were recorded at 250, 350 and 450 °C. The Lewis acidity was determined from the adsorption band at 1455 cm^{-1} and the Brønsted acidity from the adsorption band at 1545 cm^{-1} using the adsorption coefficients of Emeis [46].

2.2.1.4 X-ray photoelectron spectroscopy (XPS)

The elemental composition and the electronic state of zinc in the catalysts were determined by X-ray photoelectron spectroscopy (XPS) (AXIS Ultra, equipped with a Delay-Line-Detector (DLD) and an Al anode). The survey and multispectral were recorded at 160 eV and 20 eV pass energy, respectively.

2.2.1.5 Catalyst particle size analysis

The size of the alumina and zeolite powder particle size was determined from SEM pictures for $ZnCl_2$/H-Beta 25 $ZnCl_2$/H-Beta 150 and $ZnCl_2$/alumina by counting. In the case of the other zeolite catalysts, the size could be determined by light scattering (Malvern Zetasizer Nano-ZS) as the powders were very fine.

2.2.1.6 Transmission electron microscopy (TEM) and electron diffraction

The zinc present on the surface was determined by transmission electron microscopy (TEM) (JEOL JEM-1400Plus) using imaging and electron diffraction functions. The samples were prepared either from powder or from aqueous solution. The powder samples were prepared by blowing powder on the TEM grid with the use of a pipette. The aqueous samples were prepared by loading a 1.5 mL microtube with 0.1 mL of catalyst powder. The tube was then filled up to 1 mL with purified water. The dispersion was homogenized by shaking and exposing to 5 minutes of ultrasound. Large catalyst particles that would not be transparent to the electron beam were separated by centrifugation for 30 s at 1000 rpm. The remaining solution was diluted 1:100, transferred on the TEM grid and dried in vacuum.

For imaging an accelerating voltage of 120 kV was used, and for electron diffraction either 80 or 120 kV. To obtain the d-spacing from the electron diffraction patterns, a reference pattern (aluminum foil) was recorded at identical microscope settings. In some samples, a layer of graphene oxide was coated on the TEM grid prior to the sample deposition and used as internal calibration standard. The recorded diffraction patterns

were analyzed using the software Diffraction Ring Profiler 1.7, which was developed for phase identification in complex microstructures [47].

2.2.1.7 X-ray diffraction (XRD)

The catalyst crystal structure was determined by X-ray diffraction (XRD) with a Philips X'Pert Pro MPD using monochromatic Cu-K_α radiation. The measured 2θ range was 3.0° - 75.0° with a step size of 0.04° and a measurement time of 2.0 s per step.

2.2.2 Characterization of pure and catalyst coated microreactor platelets

The catalyst layer in the microchannels was characterized by SEM, energy-dispersive X-ray micro analysis (EDX) as described above.

2.2.2.1 Confocal white light microscopy

The surface roughness, the channel depths and the coating morphology were investigated by confocal white light microscopy using a NanoFocus μSurf. From the scans, 3D pictures and 2D profiles of the channels can be obtained. The surface roughness (S_a) was calculated from the obtained 3D-picture and is the arithmetic average of the surface roughness as given in (1),

$$S_a = \frac{1}{MN} \cdot \sum_{k=0}^{M-1} \sum_{l=0}^{N-1} \left| z(x_k y_l) \right| \qquad (1)$$

where M, and N: are the numbers of positions in x and y direction, k and 1 are indices for position along N and M and $\left| z(x_k y_l) \right|$ is the vertical deviation at position $x_k y_l$ from the mean line

The channel depths were obtained graphically from the 2D profiles of the channel.

2.2.3 Testing of catalyst coating adhesion

The coating adhesion was determined by exposing of the alumina-coated platelets to a fast nitrogen flow and six hours of ultrasonic treatment. The nitrogen flow was directed on the platelet from different angles. For the ultrasonic treatment, the platelets were placed in an empty

beaker in and ultrasonic bath. The source of ultrasound was operated in intervals of 5 s.

Furthermore, the catalyst coating stability was tested under reaction conditions for the methyl chloride synthesis. The conditions used were as follows: temperature: 573 K, 43 mL/min gas flow consisting of 4 mL/min methanol, 4 mL/min hydrochloric acid and 35mL/min helium. The high dilution of the reaction medium was chosen to avoid corrosion in the lines and the stainless steel microreactor.

2.3 Reaction setup

2.3.1.1 Gas phase analysis

The gaseous reaction mixture was analyzed by gas chromatography using an Agilent 6890N GC equipped with a flame ionization detector (FID) and an HP-Plot/U Column. (30m, I.D. 0.530 mm, film thickness: 20 µm, T=110 °C). The GC was calibrated for methyl chloride, dimethyl ether, methanol, ethanol, diethyl ether, ethylene and ethyl chloride by using mixtures of known concentrations. As no products were present in the feed, the concentrations of HCl, H_2 and water, which could not be determined by GC were calculated from the known concentrations.

2.3.1.2 Tubular fixed bed reactor

The tubular fixed bed reactor used for comparative experiments was a quartz made reactor with an inner diameter of 10 mm. The reactor is equipped with a thermocouple. Figure 3 shows the packing of the tubular fixed bed reactor. The catalyst mass in the reactor was 0.05 g for steady state experiments with and 0.12 g for transient experiments with alumina. Due to the high activity of zeolites 0.016 g of catalyst was used in this case. The catalyst bed length was 3 mm or 8 mm, respectively. The same catalyst particle size as for the microreactor was used (<32 µm). For comparing the experiments in the microreactor and tubular fixed bed reactor, the flow rate-to-catalyst mass ratio was kept constant in both reactors.

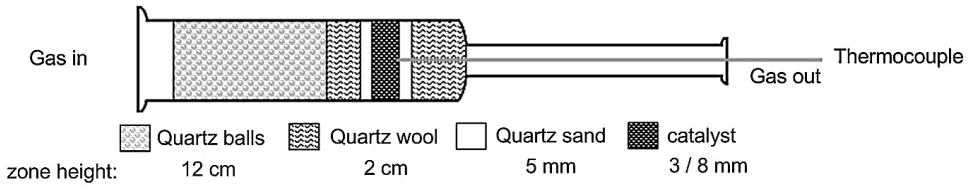

Figure 3: Schematic presentation of the tubular fixed bed reactor.

Figure 4 shows a schematic view of the experimental setup. Helium and a mixture of 20% HCl in helium (AGA, 20.000 % HCl in He) were fed from gas cylinders. The flow was controlled by mass flow controllers (Bronkhorst EL-flow). Methanol (J.T. Baker, HPLC gradient grade) was fed

from a tank containing liquid methanol using an HPLC pump (Shimadzu LC-20AD). All the lines and equipment from the methanol inlet to the GC were isolated and heated by electrical wires to 90 °C. After the reactor, a neutralization bottle filled with calcium oxide (Fischer, general purpose grade) was installed to remove HCl and water from the product gas. In this way, the corrosion problem was minimized and HCl and water injections to the GC were prevented. The temperature of the neutralization bottle was adjusted to 100 °C. At the reactor outlet, a washing bottle filled with a volume based 2:6:2 mixture of water/methanol/ethanol amine (Sigma Aldrich, ≥98%) at room temperature was placed to strip the methyl chloride from the product gas. Swagelok stainless steel lines and valves were used in the equipment. Samples were withdrawn with a gas-tight syringe through a septum in the sampling section. The syringe and an isolated transportation box were heated to 100 °C prior to sampling in order to prevent condensation of methanol. The gas samples were manually injected to the GC.

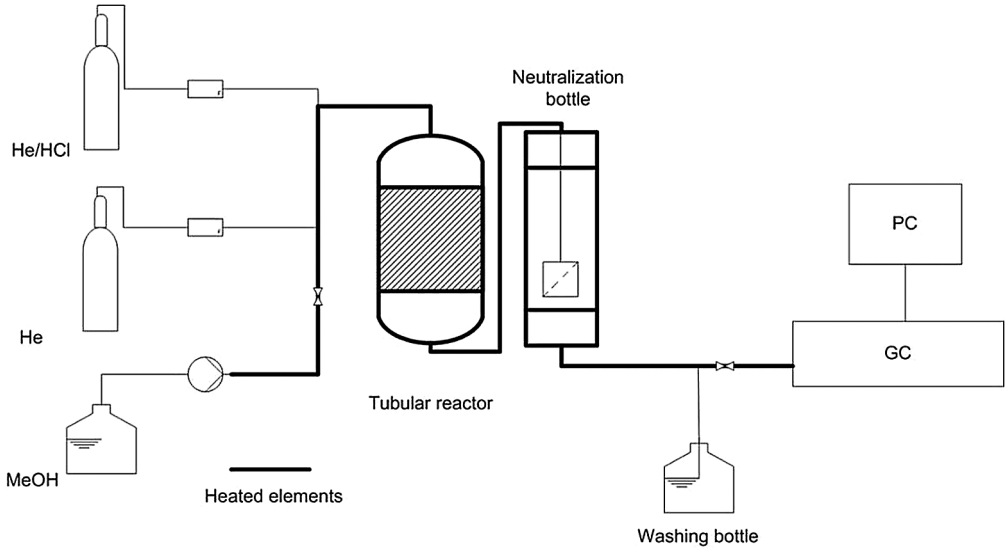

Figure 4: Experimental setup for the synthesis of methyl chloride.

2.3.2 Microreactors

The microreactor used was a stainless steel equipment made for gas-phase reactions (GPMR-mix) produced and purchased from the Institut für Mikrotechnik Mainz (IMM) (Figure 5). Technical details are summarized in Table 2.

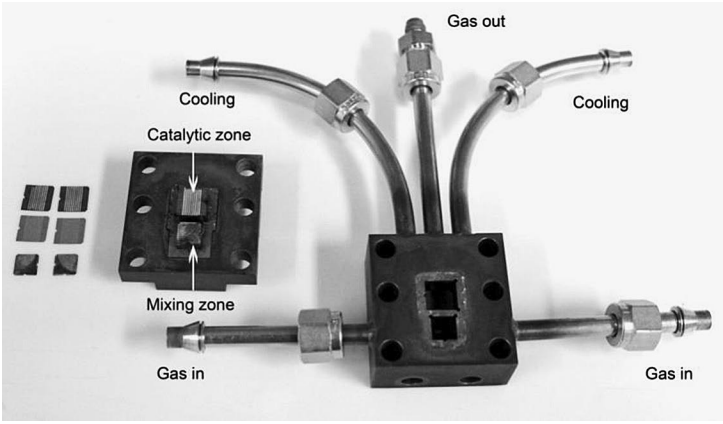

Figure 5: Microreactor with mixing and catalytic chambers.

Table 2: Technical data for the microreactor used.

Property	Value
Model	GPMR-MIX
Size (L x B x H) (mm)	45 x 45 x 32
Connectors (Inlet/Outlet)	1/4″
Standard material	Inconell 600 (2.4816) for housing and top plate; Stainless steel 1.4571 for mixing and catalyst plates
Number of mixing plates	10
Size of mixing plates (mm)	7.5 x 7.5
Channel geometry of mixing plates (width x depth) (µm)	180 – 490 x ~ 100
Number of catalyst plates	10
Size of catalyst plate (mm)	9.5 x 9.5
Channel geometry of the catalyst plates (width x depth) (µm)	460 x 95±5
Number of channels per plate	9

The microreactor consists of a mixing and a catalytic zone, each equipped with ten stainless steel microstructured platelets. The mixing plates have curved channels leading the reactants from the inlets to the mixing chamber, where they are contacted prior to entering the catalyst platelets, which have nine straight channels each. The channels are 90-100 µm deep, 460 µm in diameter and ten mm long. They had to be coated with the catalyst prior to use as described above. The reactor was heated with two heating cartridges which can be inserted in the reactor housing. The temperature in the catalyst zone was controlled by a thermocouple inserted into the microreactor through a small opening until it came in contact with the catalyst zone.

As only one inlet is needed for the second microreactor, one gas inlet was blocked with a stainless steel cylinder. Experiments for methyl chloride synthesis were carried out with an empty mixing chamber, as the steel

cylinder extended into the chamber and the mixing platelets could not be fitted. The problem was however solved so that ethanol hydrochlorination was performed with mixing platelets in the second microreactor.

A schematic overview of the reactor setup is shown in Figure 6. It corresponds to the setup for the tubular reactor. The tubular reactor was replaced by two serially coupled microreactors. A valve system with a bypass line allows sampling either after one or two microreactors. The second microreactor or the bypass lines respectively were kept under a constant nitrogen flow when not in use. Methanol hydrochlorination was conducted as described for the tubular reactor. In the case of ethanol hydrochlorination, ethanol (Etax Aa, >99.5 wt%, Altia Oy) was fed from a tank containing liquid ethanol over molecular sieves 3A. The temperatures of the lines were increased compared to methanol hydrochlorination. In ethanol hydrochlorination the evaporation line was heated to 96 °C and all the lines and equipment from the microreactors to the sampling section were heated by electrical heating wires to 106 °C.

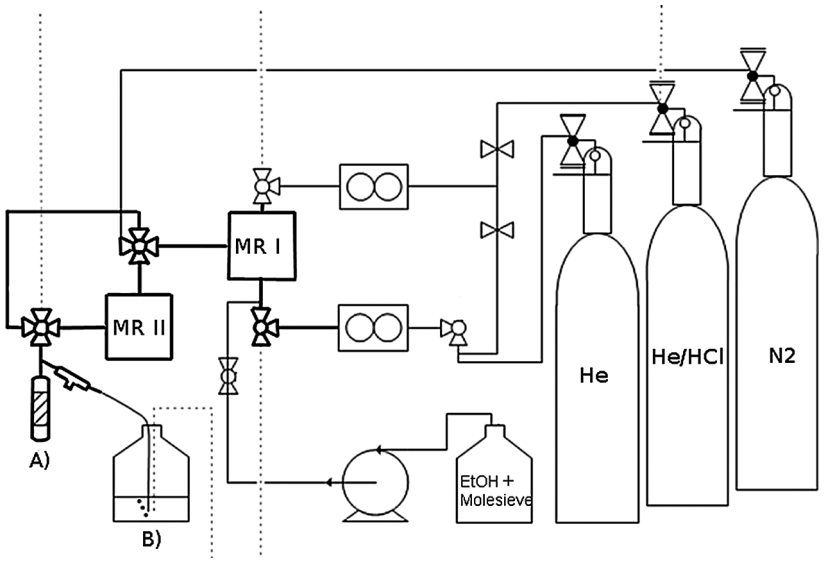

Figure 6: Schematic representation of the reaction setup. A) Neutralization bottle filled with CaO B) MeCl/EtCl trap: water/methanol/ethanolamine solution.

2.3.3 Condensation

When investigating the separation of gaseous products from the flow, the neutralization bottle was replaced by a glass-made condenser. Three different condensers were compared: An Allihn condenser with a cooling surface of 61 cm^2, a Coil condenser with 86 cm^2 of cooling surface and a Dimroth condenser with 210 cm^2 of cooling surface. An aqueous glycol solution was used as the cooling medium and the temperature varied between +1 and -15 °C. For the experiments conducted with the condensers, the mixing chamber was filled with quartz wool.

The methanol content of the liquid phase obtained from the condenser was determined using the above mentioned GC with ethanol as an internal standard. Water/methanol/ethanol mixtures of known composition were used for calibration. The water content was determined by volumetric Karl-Fischer titration and the content of hydrochloric acid was determined by titration with NaOH.

3 Results and Discussion

3.1 Catalysts [II,III]

A series of catalysts were screened for the methyl chloride synthesis: alumina, H-Beta and H-ZSM5 catalysts with varying Si/Al ratios, both neat and modified with zinc chloride.

3.1.1 Neat alumina and zeolites (II, III)

The γ-alumina used in this study has a high surface area of 280 m^2/g and a low crystallinity. It has only Lewis acid sites (LAS), which are mostly of weak and medium strengths, whereas no Brønsted acid sites (BAS) are present on the alumina. The concentrations of acid sites at different temperatures are given in Table 3. An explanation of the acid strength definition is given in the experimental part (FTIR analysis). The neat alumina catalyst had a high stability and selectivity in the methyl chloride synthesis.

Table 3: Weak, medium and strong Lewis acid sites on alumina.

	Lewis acid sites (μmol/g)
weak	73
medium	31
strong	4

Proton forms of zeolites are not suitable for the methyl chloride synthesis. The activity and selectivity are very low, as the BAS on the zeolite catalyze the production of hydrocarbons from methanol [48] and methyl chloride [49] to a considerable amount even in the presence of HCl.

3.1.2 Influence of zinc modification: support (II)

Upon modification with zinc chloride, the activity of alumina increases significantly due to the increase in number of LAS (Table 4). Zinc modified zeolites are highly active and selective in the methyl chloride synthesis. Hydrocarbon formation that was significant for proton-form zeolite was not observed after zinc modification at temperatures below 280 °C. The reason for the increased selectivity is the reduction in strong and medium BAS and the substantial increase in Lewis acid sites. Acidity profiles of neat and zinc

modified HZSM-5 are shown in Table 4. This observation is in accordance with the literature [27,28]. It can be explained by ion exchange of medium and strong acid sites, which can be vicinal BAS. Weak acid sites, being eventually isolated acid sites, are in contrast not affected by impregnation and ion-exchange.

Table 4: Brønsted and Lewis acidities of neat and $ZnCl_2$ modified catalysts.

Catalyst	Brønsted acid sites (µmol/g)				Lewis acid sites (µmol/g)			
	total	weak	medium	strong	total	weak	medium	strong
Alumina	-				107	73	31	4
$ZnCl_2$/alumina	-				147	101	36	11
H-ZSM 5 23	687	114	217	357	37	28	5	4
$ZnCl_2$/H-ZSM 5 23	155	66	44	45	412	92	116	204
H-ZSM 580	216	17	119	81	50	50	0	0
$ZnCl_2$/H-ZSM 580	89	38	33	17	237	86	76	76
H-ZSM 5280	41	8	26	7	12	12	0	0
$ZnCl_2$/H-ZSM5 280	19	5	6	8	112	49	42	21

The amount of LAS created on the supports upon modification with 5 wt% zinc varies significantly depending on the support (Table 5). Assuming that the amount or LAS created reflects the number of active zinc sites, only 0.6 mol% of the added zinc is accessible for methyl chloride synthesis on alumina, while on zeolites 1.4 mol% (H-ZSM5 280) to 5.4 mol% (H-ZSM5-23) of zinc is accessible. The lower the Si/Al ratio of the zeolites, the higher the number and strength of the obtained LAS.

Table 5: Amount of LAS created upon modification with $ZnCl_2$ and molar percent of the total zinc used during impregnation.

Catalyst	Lewis acid sites (µmol/g)	
T/°C	created	Mol% of total Zn
$ZnCl_2$/alumina	40.0	0.6
$ZnCl_2$/H-Beta 25	237.0	3.4
$ZnCl_2$/H-Beta 150	193.0	2.8
$ZnCl_2$/H-Beta 300	185.0	2.7
$ZnCl_2$/H-ZSM 5 23	375.0	5.4
$ZnCl_2$/H-ZSM 5 80	220.0	3.2
$ZnCl_2$/H-ZSM5 280	100.0	1.4

3.1.2.1 Acidity and activity of catalysts

The influence of acidity on the catalyst activity and selectivity is illustrated in Figure 7. If the conversion for the different catalysts is plotted against the number of LAS, a linear correlation is obtained for zeolite catalysts. Alumina although having a high number of acid sites, instead exhibited a considerably lower conversion. This indicates that the active sites on alumina are less active than those on zeolites, which can be explained with the lower amount of active sites originating from zinc (Table 5). The presence of some BAS on the modified zeolites could also be a reason for their high activity in methyl chloride synthesis.

The conversion increases with the total amount of LAS on the catalyst. However, the selectivity increases as well due to formation of methyl chloride from dimethyl ether. To obtain information on the selectivity depending on the catalyst acidity, the selectivity was plotted against the ratio of strong LAS to total LAS. It was revealed that the strength of the LAS influences the selectivity. The smaller the proportion of strong LAS a catalyst possesses, the higher is its selectivity. Analogously, the selectivity increases with the share of weak LAS. The selectivity is not clearly affected by medium LAS. Thus, $ZnCl_2$/alumina with its high number of weak Lewis acid sites offers a high selectivity but a low activity compared to the zeolite catalysts.

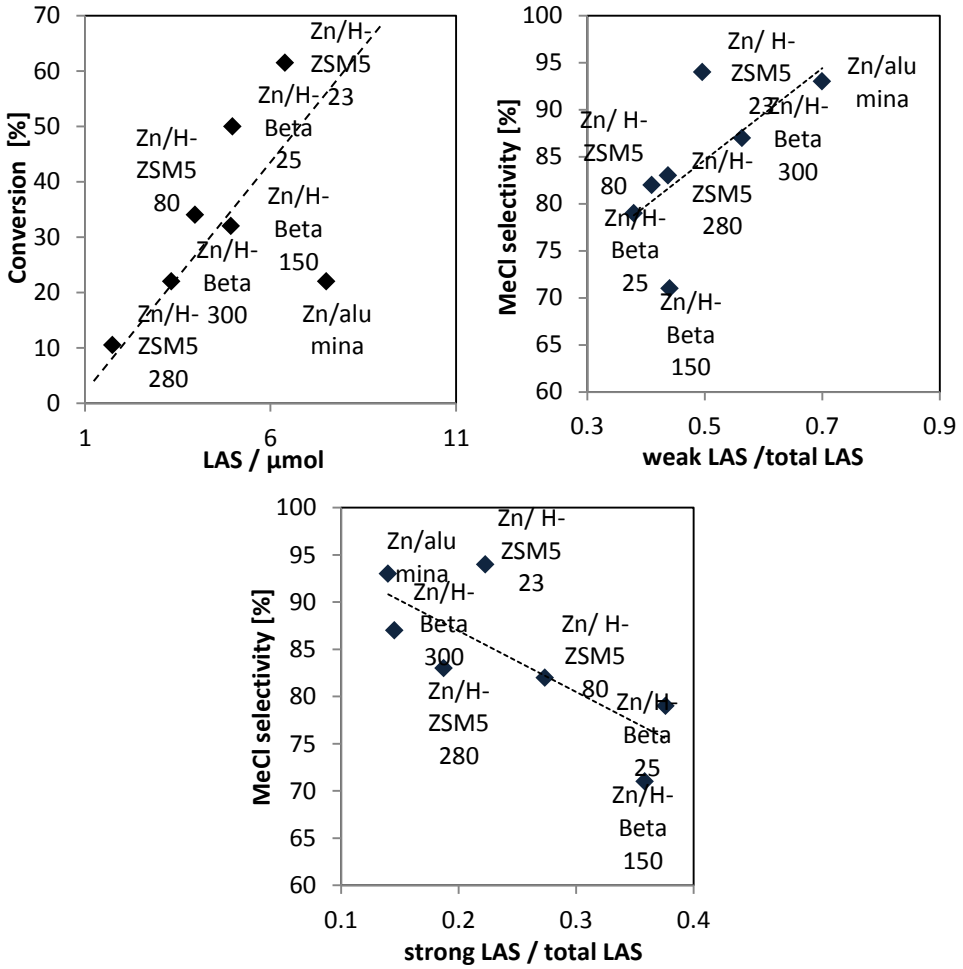

Figure 7: Correlation of the methanol conversion and methyl chloride selectivity with the Lewis acidity of the catalysts: $ZnCl_2$/alumina, $ZnCl_2$/H-ZSM5 280, $ZnCl_2$/H-ZSM5 80, $ZnCl_2$/H-Beta 25, $ZnCl_2$/H-Beta 150, $ZnCl_2$/H-Beta 300.

3.1.2.2 Catalyst stability

The catalyst stability is another important feature besides the selectivity and activity. Alumina and $ZnCl_2$/alumina were stable over 1400 min on stream, while $ZnCl_2$/H-Beta catalysts showed a considerable deactivation. The zeolites of ZSM5-type had an increased stability. No considerable deactivation was observed for H-ZSM5 280 after 1500 min time-on-stream (TOS), but the activity was very low due to its weak acidity. $ZnCl_2$/H-ZSM5 80 and $ZnCl_2$/H-ZSM5 23 are highly active and stable and thus were used in an experiment for an increased time, ca. 2200 min, to demonstrate its long-term stability. The conversion versus the time-on-stream curves for alumina, $ZnCl_2$/alumina and $ZnCl_2$/H-ZSM5 are shown in Figure 8.

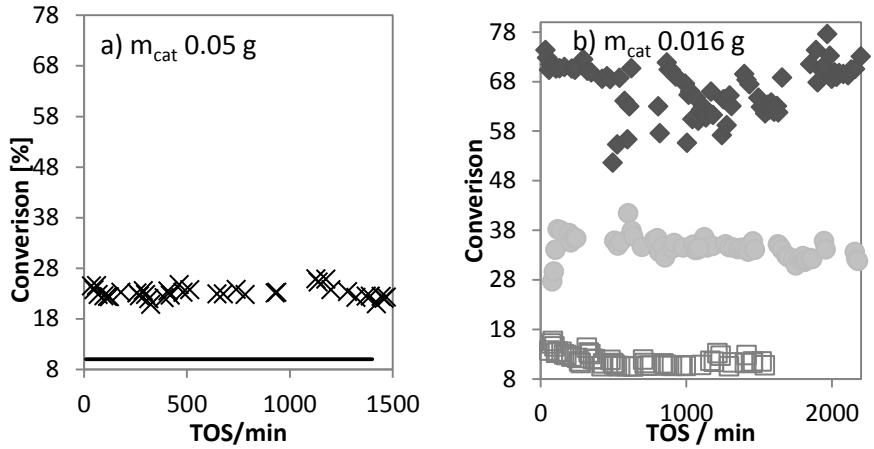

Figure 8: Methanol conversion and TOS behavior of different catalysts for methyl chloride synthesis at T= 210 °C. a) (-) alumina(calculated methanol conversion from previous experiments), (x) $ZnCl_2$/alumina, b) (♦)$ZnCl_2$/H-ZSM5 23;(●)$ZnCl_2$/H-ZSM5 80, (□)$ZnCl_2$/H-ZSM5 280.

The deactivation rate decreased with an increasing Si/Al ratio, i.e. with a decreasing acidity. One reason can be a stronger catalyst coking of highly acidic zeolites, as the carbon chain growth is more probable. It is known that methanol is transformed to dimethyl ether, an intermediate to light olefins, which can react to higher paraffins, aromatics and subsequently form coke, especially on strong acid sites [50].

Due to its higher stability and selectivity, $ZnCl_2$/alumina is principally the most suitable catalyst for the methyl chloride synthesis. However, due to the very high activity and increased stability, H-ZSM5 based materials can be potential catalysts at lower temperatures.

3.1.3 Influence of zinc modification: zinc loading on alumina (III)

The efficiencies of the zinc-modified catalysts in the methyl chloride synthesis were compared dependent on the zinc loading. Figure 9 shows that both the methanol conversion and the methyl chloride selectivity increase with zinc loading. The most significant increase of the conversion and selectivity was observed upon the first introduction of zinc. With a further increase of the zinc loading, the methanol conversion increases steadily with the zinc loading, while the selectivity does not improve further after a zinc loading of 9.4 wt %.

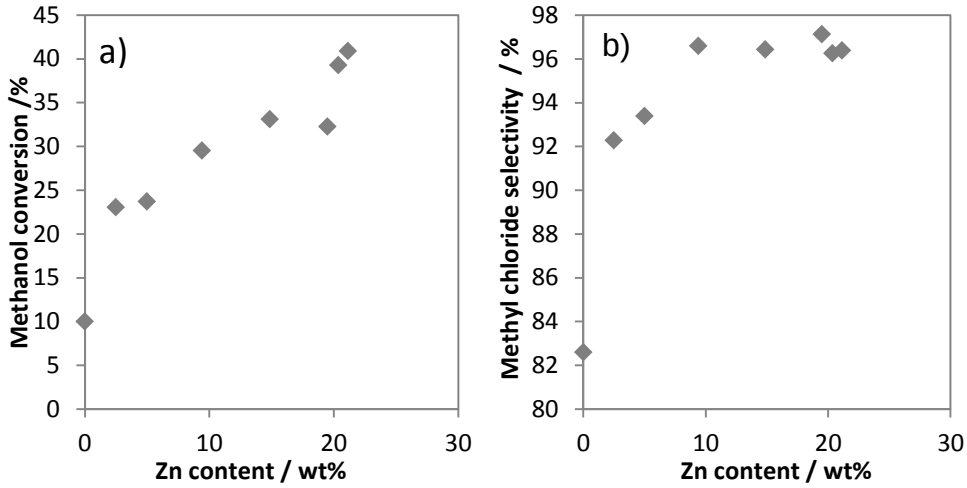

Figure 9: Influence of zinc content (wt%) on a) activity and b) selectivity of methyl chloride.

The catalyst activity can be related to the number and strength of the Lewis acid sites as shown in Figure 10. The activity decreases with an increasing number of acid sites. Therefore it can be concluded that not the number, but rather the nature of the Lewis acid sites determines the catalyst activity. The experimental data show that with an increase of the zinc loading, a shift towards more active LAS takes place. Although the absolute number and strength of Lewis acid sites decreased, the activity increased. The conversion increases with the share of weak Lewis acid sites as shown in Figure 10 b. This can be interpreted as the involvement of zinc-based Lewis acid sites which are weaker in pyridine adsorption but more active in the methyl chloride synthesis.

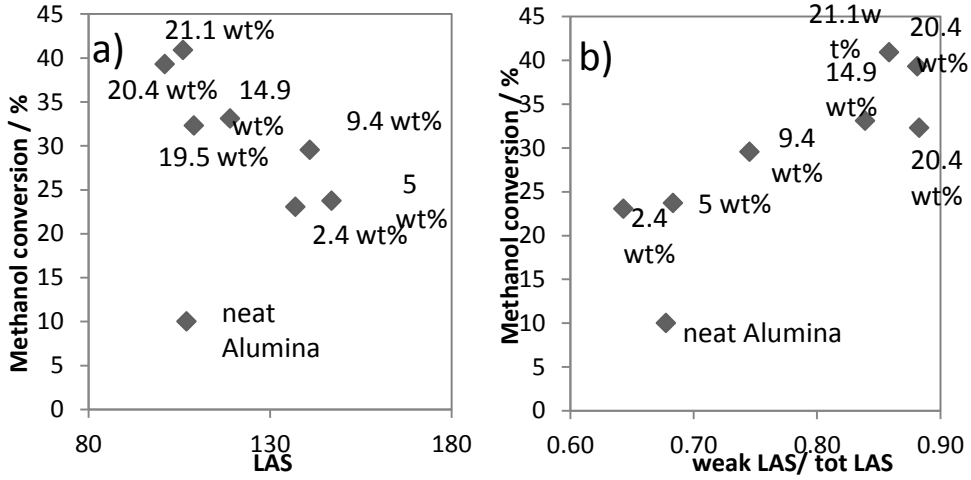

Figure 10: Influence of a) Lewis acidity and b) acid strength on activity in methyl chloride synthesis for neat and zinc-modified catalysts.

3.1.4 State of zinc on the catalyst

In all cases, the Cl/Zn atomic ratio on the prepared zinc-modified catalysts as determined by EDX and/or XPS was below 0.78. During the calcination the chlorine content is reduced due to formation of HCl gas. This indicates that most of the zinc is not present as $ZnCl_2$ on the surface but reacts with the alumina surface or forms separate particles of an oxygen-containing zinc species as ZnO or a zinc chloride hydroxide. Furthermore, chlorine can be transferred as a molecular zinc species on the surface, forming e.g. Al-O-Zn-Cl.

3.1.4.1 Crystal modification of zinc

Using X-ray-powder diffraction no crystalline zinc species could be detected, even at a zinc loading of 20 wt% on alumina. This indicates that the zinc species are amorphous. However, zinc particles can be seen by TEM on H-beta zeolites. A TEM image of zinc modified H-Beta 25 is shown in Figure 11. The zinc particle size was found to increase with a decreasing acidity of the zeolite.

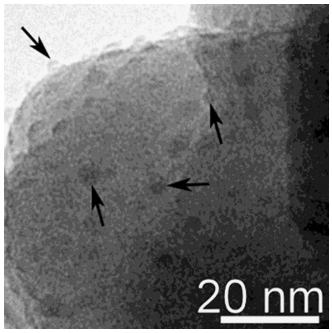

Figure 11: Transmission electron micrographs (TEM) of zinc particles on $ZnCl_2$/H-Beta 25. The arrows point towards possible zinc particles.

In the case of alumina, zinc particles were only visible when the samples are prepared from an aqueous solution. The reason is, that during the sample preparation a concentrated dispersion of alumina was used and a fraction of larger particles was removed by centrifugation. As a consequence, dissolved $ZnCl_2$ is enriched in the sample transferred to the grid, so that zinc chloride particles are visible on the alumina support starting from a loading of 9.4 wt% (Figure 12). The zinc chloride particles were not giving an electron diffraction pattern and thus are evidently not crystalline. The most abundant crystalline species observed by electron diffraction besides γ-alumina is $ZnAl_2O_4$, a spinel phase that can be formed during the calcination of the zinc modified alumina. The spinel formation has also been observed by Arndt et al. when calcining zinc oxide on alumina [51]. In two places, needle shaped crystals were found and identified as γ-$ZnCl_2$ and traces of Simonkolleite (zinc chloride hydroxide monohydrate)

were observed. The largest part of $ZnCl_2$ is visible as amorphous particles. The fact that zinc chloride particles are not visible in the dry sample can be explained by the formation of a thin layer of zinc chloride on the alumina surface that is not visible in the TEM images.

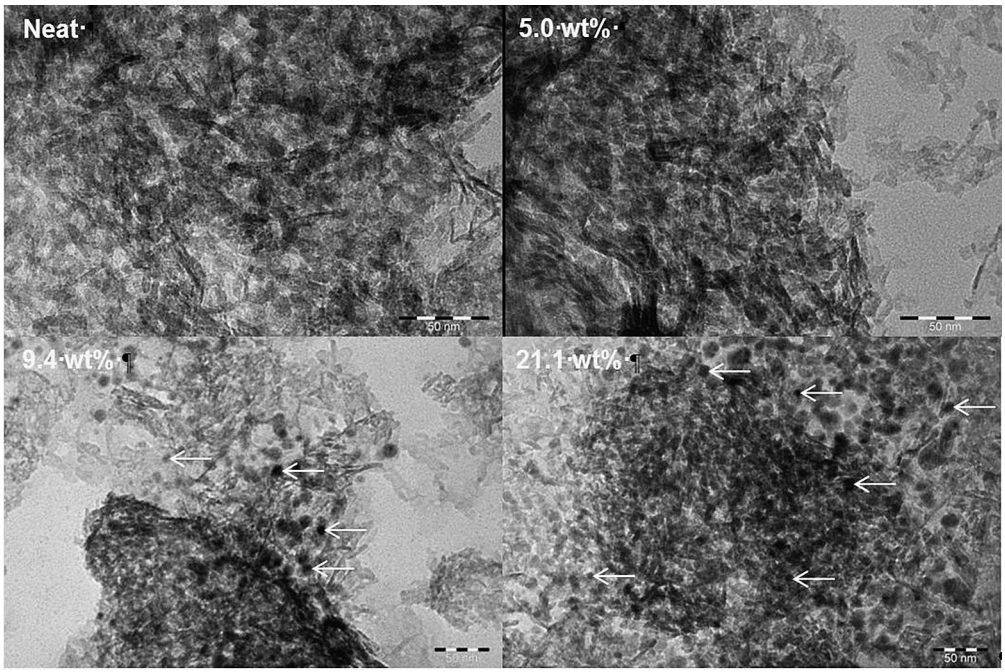

Figure 12: TEM micrographs of neat and zinc-modified alumina prepared from aqueous solution. Scale bar: 50 nm. The arrows point towards selected zinc particles for illustration.

3.1.4.2 Molecular zinc species

As indicated by the acidity profiles in the previous section, molecular zinc species should be formed on alumina and zeolites. The changes of the vibrational modes of the surface hydroxyl groups and pyridine adsorbed on alumina were investigated depending on the zinc loading. The aim was to get information on the changes of the alumina surface upon the zinc modification.

The IR-spectra of pyridine absorbed on neat and zinc-modified alumina are shown in Figure 13. It is clearly visible that neat alumina has mainly two kinds of acid sites, characterized by two peaks (1455 and 1449 cm^{-1}) for the pyridine 19b vibrational mode and two corresponding peaks for the pyridine 8a mode (1622 and 1613 cm^{-1}) [52]. According to literature, the bands at 1622 and 1455 cm^{-1} correspond to the stronger Lewis acid sites, probably tetrahedrally coordinated aluminum atoms and the modes at 1613 and 1449 cm^{-1} to weaker Lewis acid sites. Upon zinc modification, the share of the peaks at 1613 and 1445 cm^{-1} increase and they slightly shift in wavenumbers, i.e. to 1612 and 1452 cm^{-1} for 21.1 wt% zinc. The stronger Lewis acid sites vanish, which confirms that Zn^{2+} reacts with Lewis acid sites on alumina. This indicates the formation of a zinc-based active site.

In agreement with this, a decrease in intensity of OH-groups associated with weak and medium strength Lewis acid sites can be observed with increasing zinc loading. The strong Lewis acid sites are not coordinated with hydroxyl groups, so that they cannot be observed in the FTIR-spectra [56]. At higher loadings the observed OH vibrational bands are perturbed. This coincides with the visibility of zinc particles in TEM, i.e. an increased coverage of the alumina surface with bulk Zn(Cl,OH). The coverage of the surface by bulk species can be a reason for the perturbation.

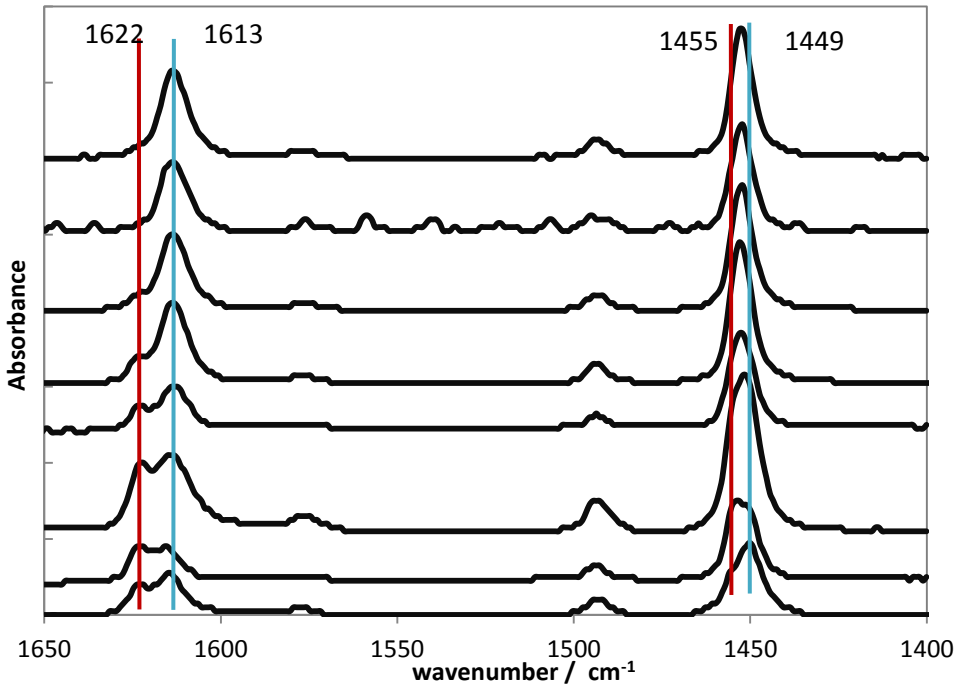

Figure 13: FTIR spectra of pyridine adsorbed on neat and zinc-modified aluminas. From top to bottom, zinc content: 21.1 wt%, 20.4 wt%, 19.5 wt%, 14.9 wt%, 9.4 wt%, 5.0 wt%, 2.4 wt%, and neat alumina. Spectra recorded at 100 °C after outgassing at 450 °C, subsequent pyridine adsorption and outgassing at 250 °C.

3.1.4.3 Influence of pH and zinc precursor

The pH of the impregnation solution or the nature of the zinc precursor, $ZnCl_2$ or $Zn(NO_3)_2$ did not significantly influence the catalyst activity and selectivity in the methyl chloride synthesis. The reason that the precursor type did not influence the activity is that the catalyst is chlorinated in-situ by the reactant HCl during the reaction. The reason for the similar activity is the reaction of the catalyst with gaseous HCl, leading to the chlorination of the alumina support [53,54]. Furthermore, $Zn(NO_3)_2$ or ZnO, formed from nitrate during the calcination, can react with HCl to form $ZnCl_2$, as has been reported by Conte et al [15]. The process results in the catalyst being almost identical to an alumina catalyst modified directly

with $ZnCl_2$. This hypothesis is also supported by the observation that spent Zn/alumina catalysts have a strongly increased Zn/Cl content of 2.52.

3.1.4.4 Catalyst of choice

Due to the higher stability and selectivity, $ZnCl_2$/alumina was the most suitable catalyst for methyl chloride synthesis according to this study. However, due to the very high activity and higher stability, H-ZSM5 based materials can be potential catalysts at lower temperatures. Working at lower temperatures is favorable for high methanol conversion and methyl chloride selectivity.

3.2 Catalyst coating (I)

3.2.1 Platelet pretreatment

The microreactor platelets were thermally pretreated to provide a catalyst coating adhesion through an increased surface roughness. The influence of the pretreatment on the surface roughness was characterized by confocal white light microscopy and scanning electron microscopy (SEM). An increase of surface roughness can clearly be seen in the SEM images of the microreactor elements (Figure 14). The surface roughness increased after the treatment from 0.1 µm initial roughness to 0.42 µm. Furthermore, an acid pretreatment was tested yielding a similar surface roughness. The platelet pretreatment showed to have not only an influence on the coating adhesion, but as well on the corrosion of the microreactor elements, which was caused by the presence of HCl and water in the reaction mixture. The iron content of the catalyst coating after the test reaction was determined by energy dispersive X-Ray analysis and the lowest amount of iron was found in the coating of the temperature pretreated elements. It was with 1.7 wt% and maximum 7 wt% at the channel borders very similar to the initial iron content on the fresh elements. Significantly higher amounts of iron, 18 wt%, were found in the coating on the acid pretreated elements. Since the heat-pretreated elements showed the best results in the catalyst adhesion and corrosion resistance, this method of pretreatment was chosen for the further work.

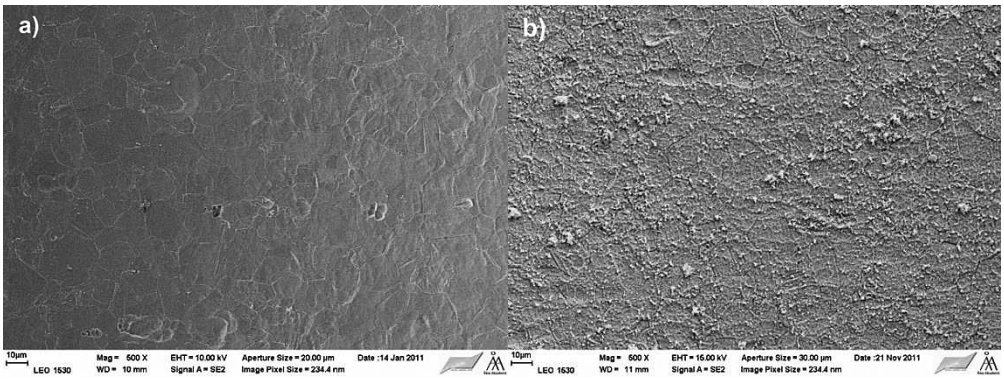

Figure 14: Scanning electron micrographs of microreactor channel surfaces; a) no pretreatment; b) after 3h thermal pretreatment at 1023 K;

3.2.2 Catalyst coating method

For catalyst coating, the slurry deposition method was selected due to its high flexibility regarding the catalytic materials. Furthermore, the channel geometry of the microreactor corresponds to a geometry found by Zapf et al. at IMM [55] to give an optimum for obtaining a uniform coating with a slurry deposition-based method. Coatings of uniform thicknesses along the channel cross-section were obtained in flat channels whereas in deep and narrow channels, the coating was non-uniform [55]. The adhesion of the catalyst layer was increased by using a finely ground catalyst powder (d_{50} = 5 µm, d_{90} = 11 µm). The addition of a binder was not necessary to obtain a stable coating.

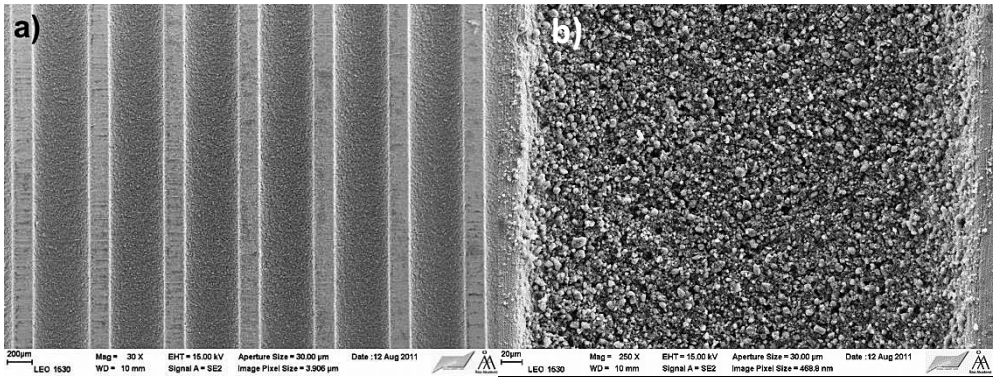

Figure 15: a) Alumina coated microchannel, top view b) close up on the catalyst layer.

A specific amount of slurry was deposited on the platelet with the aid of a Finnpipette. The amount of slurry corresponded here to the channel volume on one platelet. The quality of the coatings produced was ensured, by analyzing the morphology and thickness of the catalyst coating. These parameters are important for the flow distribution inside the microreactor. Each platelet and channel should have the same catalyst coating thickness.

3.2.3 Coating morphology

3.2.3.1 Coating thickness

The reproducibility of the coating procedure was confirmed by coating five platelets and measuring the obtained coating thickness in several channels per platelet (Figure 16). The average coating thickness was 29 µm. The variations of the coating thickness in the channels were low; a standard deviation of 3 µm, corresponding to 10% of the coating thickness was found.

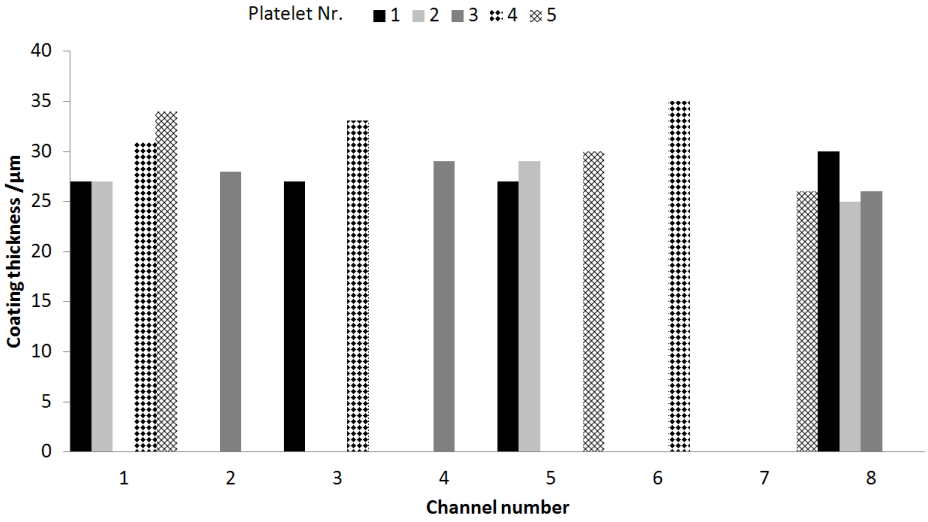

Figure 16: Coating thickness in different channels for five platelets.

3.2.3.2 Influence of drying conditions

The catalyst coating uniformity was characterized in more detail by confocal microscopy. The coating was found to be homogeneous along the channel (Figure 17 a)), whereas an increased catalyst amount was found at the channel borders, as can be seen from a 3D scan of the channel (Figure 17 b)). A reason could be drying of the coating. It starts drying from the channel ends and the catalyst particles could be transported to the borders by the drying liquid. The effect could be reduced by slowing down the drying process by drying the platelets in a fridge at 280 K. Figures 7 c) and d) show that the depth along the channel and at the channel border is uniform. Although drying still proceeds from the channel borders to the platelet inside, at lower drying speeds the catalyst particles could settle down faster than the liquid flows to the channel borders.

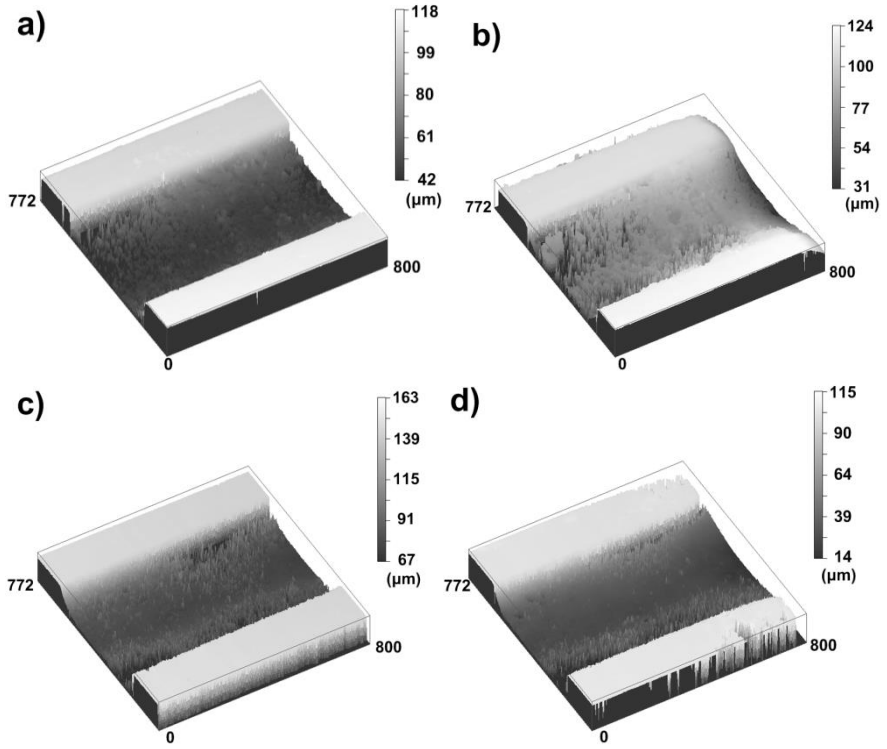

Figure 17: 3D images acquired by confocal white light microscopy: a) Microchannel middle and b) microchannel border of catalyst coated microreactor platelets, dried at ambient temperature and c) microchannel middle and d) microchannel border of catalyst coated microreactor platelets dried in a fridge.

3.2.3.3 Influence of slurry aging

The best coating characteristics with neat alumina were obtained after stirring the slurry for 4 h at 40 °C and for two days at room temperature. A shorter stirring time would lead to less uniform coatings and a longer stirring time to cracks in the coating. This effect is related to the extent of hydrolysis of alumina. The optimal time of slurry aging depends on the starting material used. In the case of the zinc modified alumina, no slurry aging was required as during the impregnation procedure the alumina was already stirred for 24 h at 80 °C in an aqueous solution. Coatings of the zinc modified alumina were of a lower quality due to the hydrolysis during the impregnation solution. The effect of the alumina hydrolysis was reported and described in detail by Meille et al. [45].

.

3.2.4 Catalyst coating stability

In order to reveal the long term catalytic stability of the thermally pretreated and alumina coated microreactor platelets a long term experiment of 45 h at 300 °C was performed. For this experiment, the

lowest flow rate adjustable with the equipment was chosen as the coke formation should be most pronounced at high conversions. As can be seen from Figure 18, the selectivity to methyl chloride and methanol conversion remained stable after an initial period over the time scale of 45 h. It should be noted here that the reaction mixture was diluted with the inert gas to prevent corrosion and that a stronger coke formation and thus a faster deactivation can be expected for more concentrated mixtures.

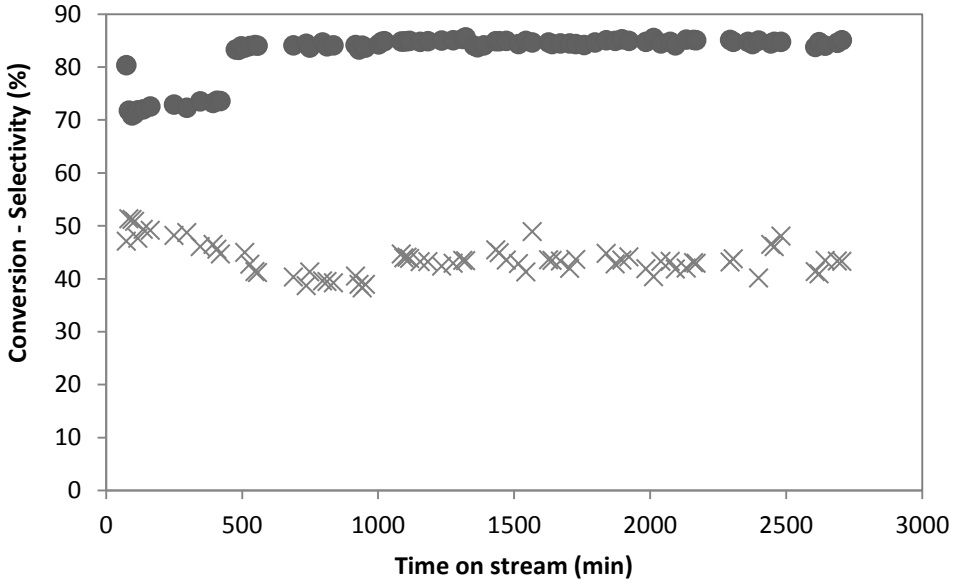

Figure 18: Methanol chlorination with HCl in the alumina coated microreactor. T=573 K, total gas flow rate:19 mL/min, 83 % Helium, 8.5 % methanol and 8.5 % HCl; (X) methanol conversion and (•) selectivity to methyl chloride.

3.2.5 Flow uniformity, catalyst coating reproducibility and kinetic experiments

For all the kinetic experiments several sets of coated platelets were used. They were coated from different batches of slurry and batches of manufactured platelets that varied somewhat in the channel depth.

Using different slurries introduces an error, as well as the use of microreactor platelets from different manufacturing batches. The original channel depth of the delivered platelets was determined to vary between 86 and 105 μm depending on the batch. However, for every set of kinetic experiments the channel depth after coating was measured and average formed to calculate the residence time.

The uniformity of the flow inside the microreactor can be visualized due to the coke formation. Figure 19 shows examples of spent microreactor platelets after the use. From the extent of the coke formation at different

positions on the platelets, conclusions on the flow distribution can be made. In general, the coke formation patterns are uniform, but in some cases certain platelets are more strongly coked than others or on a single platelet, different channels have different coke distributions. This observation indicates that the flow was not perfectly uniform. The flow maldistribution probably originate from local differences in coating thickness in the different channels. However, no dependence of the reactor performance on the set of platelets was observed when repeating the experiments at the same reaction conditions with two different set of platelets.

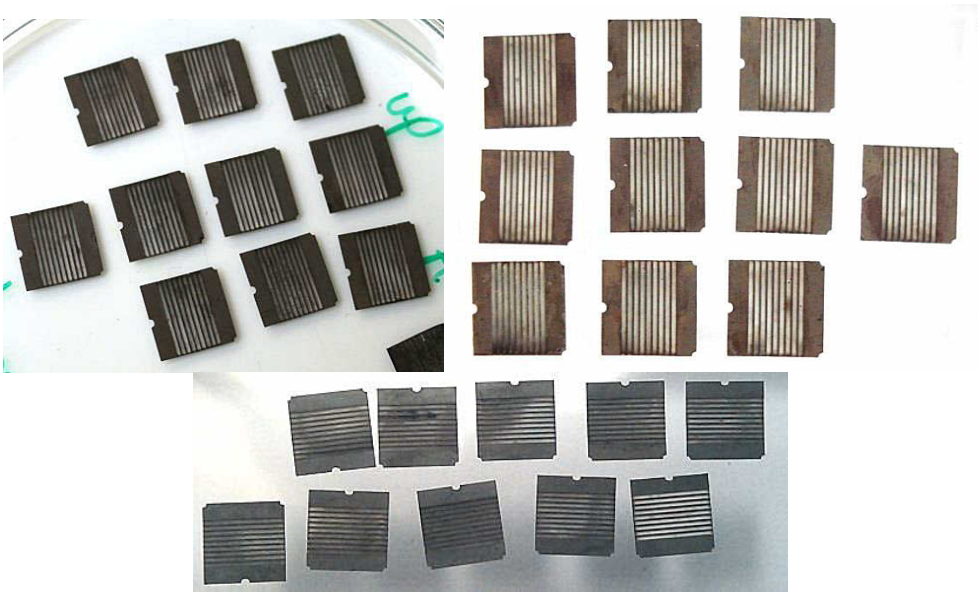

Figure 19: Different sets of microreactor platelets after use.

3.3 Kinetics and thermodynamics of methyl and ethyl chloride synthesis (IV,V)

3.3.1 Catalyst for kinetic experiments

Although $ZnCl_2$/alumina was the most active and selective catalyst, it was stable in the powder form only, placed in the quartz-made tubular reactor. When the zinc modified alumina was coated on microreactor platelets a constant decline of the product selectivity was observed, while the activity remained stable. A reason for this can be the leaching of iron into the coating modifying the zinc-active sites. Thus, for the systematic kinetic experiments neat alumina was used.

3.3.2 Kinetics, thermodynamics and diffusion limitations of methyl chloride synthesis (IV)

The experiments with methanol hydrochlorination were conducted in a single microreactor and in a quartz-made tubular reactor on neat γ-alumina.

3.3.2.1 Thermodynamics

The equilibrium constants for reactions (I)-(III) (see Introduction) were calculated with HSC7 software (Antti Roine, Outotec Research Oy) using the Gibbs energy minimization method.

The methanol conversion and the selectivity to methyl chloride in the thermodynamic equilibrium considering reactions (I)-(III) were obtained from simulating all reactions simultaneously with ModEst 6.1 Software (Profmath Oy), assuming equimolar feeds of MeOH and HCl and a product free initial state. The results are summarized in Table 6.

Table 6: Temperature dependent equilibrium MeOH conversion and equilibrium selectivity to MeCl .

T [°C]	K_1	K_2	K_3	MeOH conversion	Selectivity to MeCl
280	500.4	13.03	38.40	0.969	0.973
290	445.6	11.99	37.18	0.967	0.971
300	398.4	11.06	36.03	0.965	0.970
310	357.6	10.23	34.94	0.963	0.969
320	322.1	9.49	33.92	0.961	0.968
330	291.2	8.84	32.96	0.959	0.967
340	264.1	8.24	32.04	0.957	0.966

Table 6 reveals that all reactions should be treated as reversible. The conversion of methanol to methyl chloride (I) in the temperatures range 280-340 °C is about 96-97%. Lower temperatures are favorable for a higher conversion and a higher selectivity in the thermodynamic equilibrium. All reactions are lightly exothermic with a reaction enthalpy of ca. 30 kJ/mol at 300 °C.

3.3.2.2 Conversion and selectivity

Concentration profiles for methyl chloride synthesis were recorded for temperatures between 280 °C and 340 °C at an HCl/MeOH ratio of 1:1. Furthermore, the total reactant concentration and the HCl/MeOH ratio were varied.

The influence of the temperature and the residence time on the methanol conversion is shown in Figure 20. Conversions from 4 % to 83 % were achieved in the microreactor. Higher conversions within the studied temperature range could not be obtained due to limitations of the equipment (flow controllers). The selectivity of the reaction was around 80-90% and increased with the methanol conversion. The selectivity was rather independent of the reaction temperature, suggesting similar activation energies for methyl chloride and dimethyl ether formation.

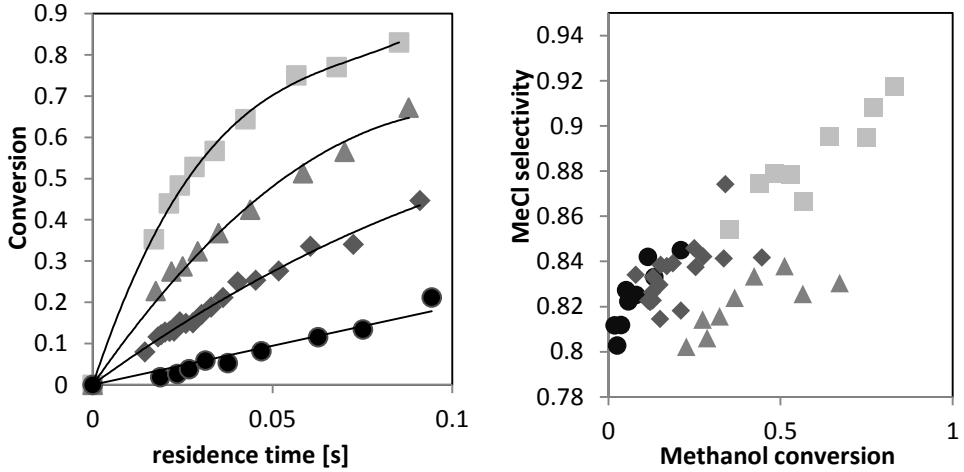

Figure 20: Influence of temperature and residence time on methanol conversion in microreactor and dependence of methyl chloride selectivity on temperature and methanol conversion. (■) 340 °C; (▲) 320 °C; (♦) 300 °C; (●) 280 °C.

3.3.2.3 Comparison of with tubular fixed bed reactor and microreactor

Combined concentration profiles at 300 °C in the microreactor and the tubular fixed bed reactor are shown in Figure 21. Several conclusions could be made from the analysis of the combined data. First, it can be seen that the data from the microreactor and the tubular reactor overlap, suggesting that both reactors operated in the kinetic regime. This observation allows combining both data sets for kinetic modeling. The microreactor reveals in a very detailed way the behavior at low conversions far from the equilibria of reactions (I) and (II), while the tubular fixed bed reactor gives information on the system behavior at higher conversions, on the influence of the reactant adsorption and also on reaction (III), which can be directly observed at high conversions only. In the microreactor, the dimethyl ether concentration is only increasing, but at the high conversions achieved in the tubular reactor, the decline of the dimethyl ether concentration can be observed. Dimethyl ether shows therefore a typical behavior of a reaction intermediate. The data obtained from the tubular fixed bed reactor are a useful completion of the microreactor data.

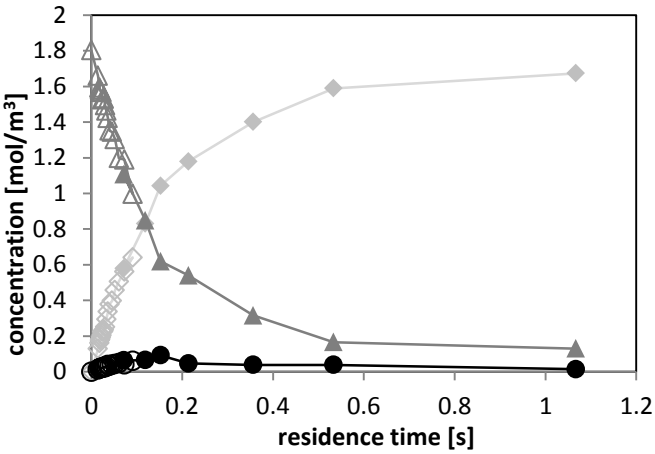

Figure 21: Combined results from microreactor and tubular fixed bed reactor. (●/○) DME; (▲/△) MeOH; (♦/◇) MeCl. Open symbols represent the data from the microreactor and closed symbols the data from the tubular fixed bed reactor.

3.3.2.4 Kinetic modelling

The kinetic model was based on the Langmuir-Hinshelwood mechanism, i.e. on the reactions between adsorbed species on an ideal surface. Stronger adsorption is expected for H_2O, MeOH, MeCl and HCl compared to DME. As HCl and methanol both adsorb on one unit of [Al-O] [56,57], competitive adsorption is assumed and [Al-O] as active site is represented in the following as (*). Water and methyl chloride were assumed to adsorbed on the same active site.

According to this information on the reactant and product adsorption, a reaction mechanism is proposed as displayed in Scheme 1, where $N^{(i)}$ denote the stoichiometric numbers of the surface steps giving the overall reactions (I)-(III)). The surface reactions (1)-(3) in Scheme 1 are assumed to be the rate determining steps. A plug flow model was used to describe the reactors.

Scheme 1: Proposed reaction mechanism.

	$N^{(I)}$	$N^{(II)}$	$N^{(III)}$
$CH_3OH + * \leftrightarrow CH_3OH*$	1	2	-1
$HCl+* \leftrightarrow HCl*$	1	0	1
$CH_3OH* + HCl* \leftrightarrow CH_3Cl* + H_2O*$ **rds (1)**	1	0	0
$CH_3OH* + CH_3OH* \leftrightarrow CH_3OCH_3* + H_2O*$ **rds (2)**	0	1	0
$CH_3OCH_3* + HCl* \leftrightarrow CH_3OH* + CH_3Cl*$ **rds (3)**	0	0	1
$H_2O* \leftrightarrow H_2O + *$	1	1	0
$CH_3Cl* \leftrightarrow CH_3Cl + *$	1	0	1
$CH_3OCH_3* \leftrightarrow CH_3OCH_3 + *$	0	1	-1

An ODE solver (Odessa) was used to solve the differential equations and parameters were optimized by the Levenberg-Marquardt and the Simplex algorithms. The least squares method was used to obtain the minimum of the objective function.

In order to determine the activation energy and the pre-exponential factor for the reactions, k was expressed with the Arrhenius law. To suppress the numerical correlation between A_i and E_{Ai}, the substitution $(1/T\text{-}1/T_{mean})$ is introduced and $k_{i,mean}$ thus represents the rate constant at the average temperature. The real pre-exponential factor is calculated after the regression.

$$k_i' = k_{i,mean} \cdot e^{\frac{-E_{ai}}{R}(\frac{1}{T}-\frac{1}{T_{mean}})} \qquad (2)$$

Based on Scheme 1, the rate equations were expressed as follows:

$$r_1 = k'_1 \frac{c_{MeOH}c_{HCl} - \frac{c_{MeCl}c_{H2O}}{K_I}}{D} \qquad (3)$$

$$r_2 = k'_2 \frac{c_{MeOH}^2 - \frac{c_{DME}c_{H2O}}{K_{II}}}{D} \qquad (4)$$

$$r_3 = k'_3 \frac{c_{DME}c_{HCl} - \frac{c_{MeCl}c_{MeOH}}{K_{III}}}{D} \qquad (5)$$

$$D = (K_{MeOH}c_{MeOH} + K_{HCl}c_{HCl} + K_{MeCl}c_{MeCl} + K_{H2O}c_{H2O} + 1)^2$$

The kinetic model as given in equations (3)-(5) was not directly used to fit the data as it is over-parameterized. The adsorption parameters were in the first stage estimated separately to get information about the relevance of the adsorption constant for each component. Only the adsorption constants of methanol and HCl showed to have a value significantly different from zero. Thus, water and methyl chloride adsorption were not considered in further the modeling. The following different expressions for the adsorption term were compared:

$$D=1 \quad (6)$$

$$D=(1+K_{MeOH}*c_{MeOH})^2 \quad (7)$$

$$D=(1+ K_{HCl}*c_{HCl})^2 \quad (8)$$

$$D=(c_{HCl} + \beta c_{MeOH})^2 \quad (9)$$

In eq. (9) the parameter β describes the ratio of the adsorption constants of HCl and methanol.

For description of the temperature dependence a model with D=1 is sufficient to describe the data accurately. However, to describe the experimental observations when varying the MeOH:HCl ratios, adsorption terms have to be considered. The best result was obtained for $D=(1+ K_{HCl}*c_{HCl})^2$. However if the reaction is performed in an excess of methanol, the expression $D=(1+K_{MeOH}*c_{MeOH})^2$ is more accurate. In Figure 22 the model predictions and experimental data for methyl chloride and dimethyl ether concentration profiles are shown. The kinetic parameters are summarized in Table 7.

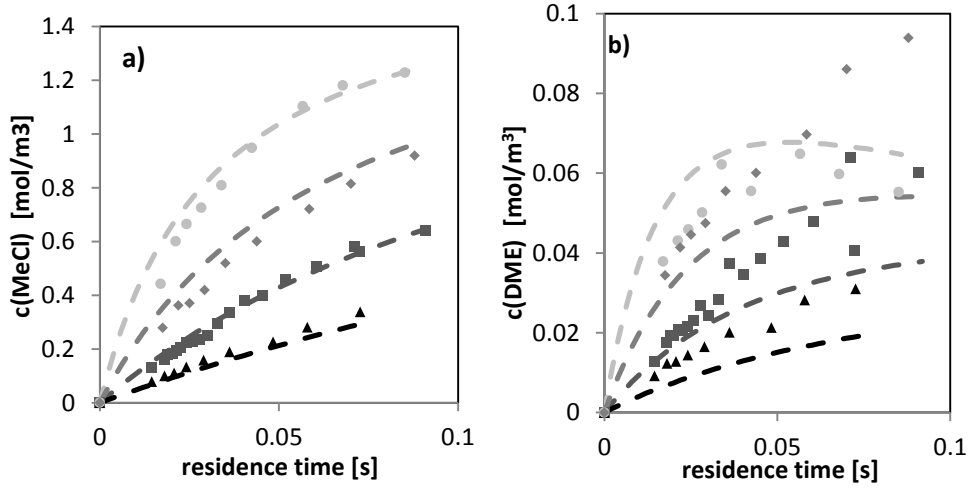

Figure 22: Temperature dependence of MeCl and DME formation; (●) 340 °C; (♦) 320 °C; (■) 300 °C ; (▲) 280 °C.

Table 7: Kinetic parameters of reactions (I), (II) and (III), R^2=99.6; *: fixed values

Parameter	Value	Error /%
A_1 [$m^3 \cdot mol^{-1} \cdot s^{-1}$]	$3.33*10^{10}$	4.5
A_2 [$m^3 \cdot mol^{-1} \cdot s^{-1}$]	$2.73*10^{10}$	3.3
A_3 [$m^3 \cdot mol^{-1} \cdot s^{-1}$]	33500	*
E_{a1} [kJ/mol]	108	1.5
E_{a2} [kJ/mol]	118	2.6
E_{a3} [kJ/mol]	36	*
K_{HCl}	0.116	13.6

The activation energy for reaction I is about twice higher than the values published previously. An overview of the reported activation energies of reactions (I) and (II) along with the catalyst particle sizes used is given in Table 8. It is worth mentioning that for reaction (II), which is about ten times slower than reaction (I), the activation energy obtained in this work is similar to the ones reported in literature [29,58]. For these reasons, it is assumed that the differences in the activation energies reported in literature are caused by the presence of internal diffusion limitations in the catalyst pores. With the catalyst layer thickness of 13-18 µm, the catalyst used in this study is significantly thinner than those previously used. Furthermore, the layer can be considered as a macroporous array of catalyst particles with d_{50} = 5 µm and d_{90} = 11 µm.

Table 8: Activation energies and particle sizes for reactions (I) and (II) as published in literature.

Author	Activation Energy [kJ/mol] Reaction (I)/ (II) /	Particle Size [µm]
Schlosser et al (1970)	(I)56.5	100-300
Svetlanov and Flid (1966)	(I)53.2	100-300
Svetlanov and Flid (1966)	(II)91.3	100-300
Becerra et al (1992)	(I)54.4	250
Thyagaran et al (1966)	(I) 80.16	1000
Lee et al. (2006)	(II) 115	100-250

3.3.2.5 Reaction and diffusion in the porous catalyst layer

To confirm the presence of diffusion limitations and explain the differences in activation energies observed by us and previous studies, the internal diffusion in the catalyst layer was mathematically modeled. For the evaluation of the diffusion in the porous catalyst layer, the mean transport pore model was used.

The data obtained from the microreactor system were assumed to represent the intrinsic kinetics, and the above presented kinetic model and parameters were used in the simulation of the reaction-diffusion model for catalyst layers.

The thickness of the catalyst layer was varied between 15 and 2000 µm. The smallest layer thickness represents the microreactor and the largest thickness corresponds to the conventional fixed bed reactor. The intermediate values of 200-300 µm correspond to typical experimental conditions of previous investigators (Table 8). The temperature range of the simulation was 280-340 °C. The simulation results for the methanol concentration profiles in the catalyst layer at 300 °C and reactant concentrations of 2.5 mol/m³ are displayed in Figure 23. The corresponding effectiveness factors are reported in Table 9.

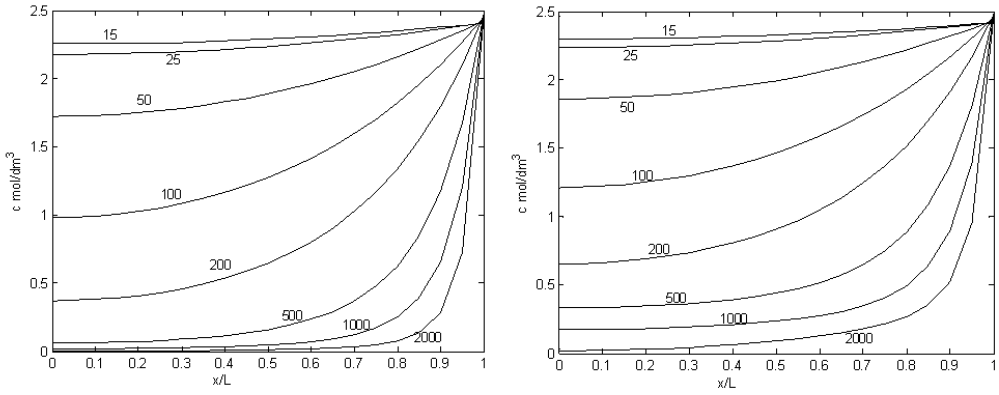

Figure 23: Concentration profile of a) methanol and b) HCl inside the catalyst layer for different thicknesses. T = 300 °C. The numbers represent the layer thickness (in micrometer).

Table 9: Effectiveness factors η of methanol and HCl for different catalyst layer thicknesses. Conditions as in Figure 17.

Catalyst layer thickness [µm]	Effectiveness factor ηMeOH	Effectiveness factor ηHCl
15	0.91	0.93
25	0.87	0.90
50	0.69	0.73
100	0.42	0.46
200	0.22	0.24
500	0.09	0.10
1000	0.05	0.06
2000	0.03	0.04

The simulation confirms that the reaction is strongly influenced by diffusion for layer thicknesses starting from of 50 µm (Figure 23 and Table 9). Experimental results in the current work were, with an effectiveness factor exceeding 0.9, obtained within the kinetic regime. The effectiveness

factor for HCl is slightly higher than for MeOH, as it is only consumed in reaction (I), whereas methanol takes part in reactions (I) and (II). The particle thickness typically used in conventional fixed bed reactors (1000-2000 μm) implies a considerable internal diffusion resistance, where the MeOH concentration drops down close to 0 inside the catalyst layer. For the intermediate layer thicknesses (100-300 μm) used in previous laboratory scale experiments (Table 8), the internal diffusion plays a role, suppressing the effectiveness factor. This explains the differences in apparent activation energies obtained by us and the previous investigators.

In the case of a heavy internal diffusion resistance, the effectiveness factor is proportional to the reciprocal Thiele modulus, $\eta_{ei} = 1/\varphi_i$ where $\varphi_i = \sqrt{\frac{kc_i^{n-1}}{D_{ei}}} R_L$. The experimentally observed rate is $r'_i = \eta_{ei} k c_i^n$ which implies that r_i' is proportional to $\sqrt{k} = \sqrt{Ae^{-Ea/(RT)}}$ and the apparent activation energy is ½ E_A in the extreme case observing that the diffusion is only weakly activated by temperature. This can explain the factor two between the obtained and the previously published activation energies.

3.3.3 Kinetic modeling of ethyl chloride synthesis (V)

The experiments with ethanol hydrochlorination were conducted in two serially coupled microreactors on neat γ-alumina.

3.3.3.1 Thermodynamics

In Table 10 the equilibrium constants for the reactions (see Introduction) are given. It is clear that the reactions cannot be kinetically modeled as irreversible. Furthermore it has to be noted, that only four reactions are thermodynamically independent. Reactions (I), (II) and (VI) are related according to: $K_{II}=K_I/K_{VI}$. Reactions (I), (III) and (VII) are related according to $K_I=K_{III}/K_{VII}$ and reactions (II), (III) and (IV) are related by $K_{II}=K_{III}/K_{IV}$.

Table 10: Temperature dependent equilibrium constants of reactions (I)-(VII); equilibrium conversions and selectivities.

Temperature / °C Equilibrium constant	240	260	280	300	320	340
K_I	363.0	287.6	231.7	189.6	157.3	132.0
K_{II}	7.9	6.6	5.6	4.8	4.2	3.7
K_{III}	109.9	165.7	242.5	345.7	481.2	655.5
K_{IV}	13.8	25.0	43.1	71.6	114.7	178.0
K_V	0.1	0.2	0.4	0.7	1.1	1.8
K_{VI}	45.7	43.3	41.2	39.2	37.5	35.9
K_{VII}	0.3	0.6	1.0	1.8	3.1	5.0
EtOH conversion	99.1	99.1	99.1	99.2	99.2	99.2
EtCl selectivity	77.6	75.9	74.1	72.3	70.4	68.4
C_2H_4 selectivity	20.8	22.4	24.1	25.9	27.7	29.5
C_2H_4O selectivity	1. 5	1.6	1.7	1.8	1.9	2.0
DEE selectivity	0.07	0.06	0.05	0.05	0.04	0.04

The equilibrium conversion is higher than 99 % for all temperatures, the main product being ethyl chloride with selectivities varying between 77.6 and 68.4% depending on the reaction temperature. Ethylene is the second most important product with selectivities varying between 20.8 and 29.5%. With an increasing temperature, the ethyl chloride selectivity in equilibrium decreases, while the ethylene selectivity increases. Small amounts of acetaldehyde are predicted to be present, while the diethyl ether selectivity is negligible at the equilibrium.

3.3.3.2 Conversion and selectivity

In Figure 24 the dependence of the ethanol conversion on the residence time is shown at temperatures ranging from 240 to 340 °C. The data at low residence times were obtained from samples withdrawn after one microreactor (filled symbols) and at higher residence times after two microreactors (empty symbols). At intermediate residence times, the data from both microreactors are overlapping. The data from one and two microreactors, i.e. filled and empty symbols, overlay very well as revealed by Figure 24. These results confirm that the serial coupling of the two microreactors does not lead to any side effects. The data obtained from two microreactors at 300 °C indicate slightly higher conversions, which could be explained by the reaction taking place to a small extent in the mixing channels of the second microreactor at elevated temperatures. The reaction of HCl with the metal surface leads to the formation of metal chlorides which can be active in the ethyl chloride synthesis. A maximum ethanol conversion of 98.6 % can be reached at 340 ºC at a residence time of 0.15 s.

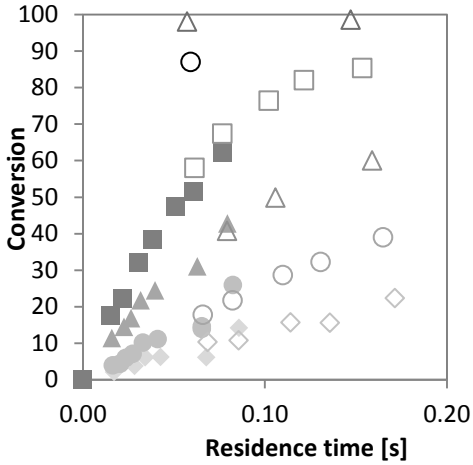

Figure 24: Influence of temperature and residence time on ethanol conversion. (Δ) 340 °C, (o) 320 °C, (■)300 °C, (▲) 280 °C, (●) 260 °C, (♦) 240 °C. Filled symbols: one microreactor, empty symbols: two microreactors.

The selectivity of the reaction at different temperatures to ethyl chloride, diethyl ether ethylene and acetaldehyde is shown in Figure 25. The selectivities are plotted against the ethanol conversion for a better comparability of the experimental data at different temperatures and to demonstrate the roles of the intermediate products.

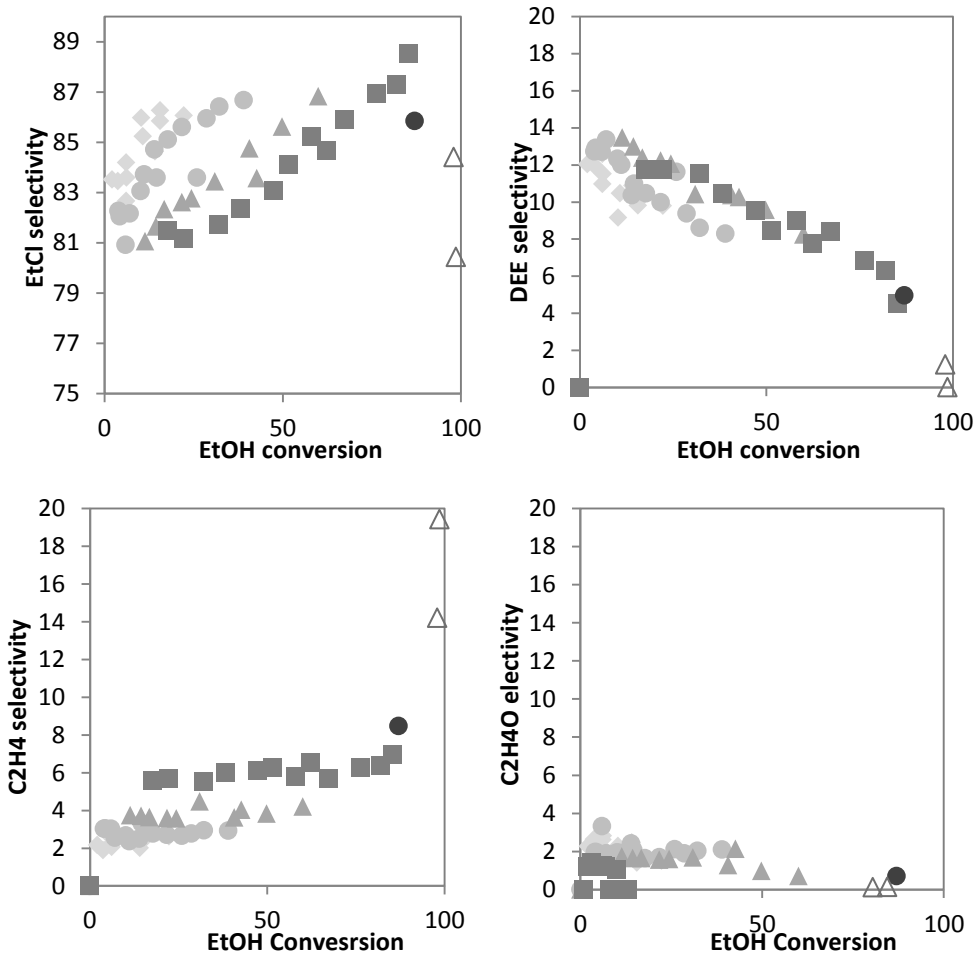

Figure 25 Influence of temperature on selectivity to a) ethyl chloride, b) diethyl ether, c) ethylene and d) acetaldehyde dependent on ethanol conversion: (Δ) 340 °C, (●) 320 °C, (■) 300 °C, (▲) 280 °C, (●) 260 °C, (♦) 240 °C.

The ethyl chloride selectivity exceeded 80 % for all the temperatures and residence times, i.e. conversions screened. The diethyl ether selectivities were 0-13 %, while the ethylene selectivities were in the range of 2-6%. The selectivity to acetaldehyde was always less than 4%. The ethyl chloride selectivity increased with conversion while the diethyl ether selectivity decreased indicating that diethyl ether is an intermediate product which is converted to ethyl chloride according to reaction (VI).

With an increasing temperature, the selectivity to ethyl chloride at a constant conversion decreases. Furthermore, the ethyl chloride selectivity decreases with the ethanol conversion at 340 °C. At the same time the ethylene selectivity increases, which suggests that at high temperatures, ethyl chloride is converted to ethylene as reflected in the thermodynamic equilibrium compositions (Table 10). A low amount of ethylene and the stable ethylene selectivity with the ethanol conversion in kinetic experiments below 340 °C show that the formation of ethylene from ethyl

chloride is very slow at lower temperatures. Nevertheless, a minor increase of the ethylene selectivity can be observed, e.g. 5.6 % at 17.6% conversion to 7.0 % at 85.3 % conversion at 300 °C. In conclusion, a high selectivity to ethyl chloride can be obtained at a low temperature and a controlled residence time. If the thermodynamic equilibrium is approached, the ethylene content will increase to ca 20-30 %, depending on the temperature. In the investigated range the highest ethyl chloride selectivity of 88.5 % was obtained at 300 °C at a conversion of 85.3 %. From the trend in Figure 25a it can be expected that the selectivity can be further increased by increasing the residence time. The disproportionation of diethyl ether to ethylene and ethanol was not observed. The diethyl ether and acetaldehyde selectivities were slightly lowered with a decreasing temperature, in favor of the ethyl chloride and ethylene selectivities.

The HCl:EtOH ratio was varied to reveal the influence of the adsorption processes on the catalyst. Kinetic experiments at the following initial HCl:EtOH ratios were conducted: 2.00:0.98, 1.91:1.88, 2.53:2.51, 1.76: 3.50. An excess of HCl favored the ethyl chloride formation and the ethylene production, while the diethyl ether production was suppressed. This is an effect of the HCl and ethanol amounts adsorbed on the alumina. The reason is that diethyl ether formation requires two neighboring ethanol molecules on alumina. Consistently, upon introduction of an excess of ethanol, the diethyl ether selectivity was increased and the selectivities to the other products was lowered. Introduction of a higher reactant concentration, keeping the HCl:EtOH ratio at 1:1, increased the ethyl chloride production and lowered the ethylene production. The diethyl ether production was not affected. No clear trends were observed for the acetaldehyde selectivity, as the concentrations were very low, i.e. 100-fold less than the ethyl chloride concentrations and thus the relative analytical error was high.

3.3.3.3 Reaction mechanism

The reaction mechanism of ethanol hydrochlorination as used for the kinetic modeling is summarized in Scheme 2. Reactions (IV) and (VII), i.e. ethylene formation from diethyl ether (IV) and from ethyl chloride (VII) are not considered in the kinetic model. The reason is that in the temperature range for the kinetic modeling (240 – 300 °C) the ethylene selectivity is nearly constant, which indicates that these reactions are not taking place to significant extent under these conditions. The reaction mechanism is based on the principle of an ideal surface and surface reactions between adsorbed species. The surface reactions (I)-(VI) are assumed to be the rate determining steps, while the adsorption and desorption steps are presumed to be in quasi-equilibria.

Scheme 2: Proposed reaction mechanism.

	$N^{(I)}$	$N^{(II)}$	$N^{(III)}$	$N^{(V)}$	$N^{(VI)}$
$C_2H_5OH + * \leftrightarrow C_2H_5OH*$	1	2	1	1	-1
$HCl+* \leftrightarrow HCl*$	1	0	0	0	1
$C_2H_5OH*+ HCl* \leftrightarrow C_2H_5Cl* + H_2O*$ rds (I)	1	0	0	0	0
$C_2H_5OH* + C_2H_5OH* \leftrightarrow C_2H_5OC_2H_5* + H_2O*$ rds (II)	0	1	0	0	0
$C_2H_5OH* + * \leftrightarrow C_2H_4* + H_2O*$ rds (III)	0	0	1	0	0
$C_2H_5OH* + * \leftrightarrow C_2H_4O* + H_2*$ rds (V)	0	0	0	1	0
$C_2H_5OC_2H_5* + HCl* \leftrightarrow C_2H_5OH* + C_2H_5Cl*$rds (VI)	0	0	0	0	1
$H_2O* \leftrightarrow H_2O + *$	1	1	1	0	0
$C_2H_5Cl* \leftrightarrow C_2H_5Cl + *$	1	0	0	0	1
$C_2H_5OC_2H_5* \leftrightarrow C_2H_5OC_2H_5 + *$	0	1	0	-1	0
$C_2H_4* \leftrightarrow C_2H_4 + *$	0	0	1	0	0
$C_2H_4O* \leftrightarrow C_2H_4O+ *$	0	0	0	1	0

3.3.3.4 Kinetic model

The software Matlab was used for regression of the kinetic parameters. As for methyl chloride, the internal diffusion limitations in the microreactor were considered to be negligible. The kinetic and the adsorption constants were expressed by the Arrhenius and the van't Hoff equations, respectively. A plug flow model was used for the microreactor. The modeling strategy was similar to the case of methyl chloride.

Comparing the different adsorption terms showed that ethanol and HCl adsorption were important for the kinetic model. Modeling the water adsorption did not improve the predictions and was not taken into account in further modeling efforts. The rate equations were written as follows:

$$r_1 = k'_1 \frac{c_{EtOH} c_{HCl} - \frac{c_{EtCl} c_{H2O}}{K_I}}{D} \quad (10)$$

$$r_2 = k'_2 \frac{c_{EtOH}^2 - \frac{c_{DEE} c_{H2O}}{K_{II}}}{D} \quad (11)$$

$$r_3 = k'_3 \frac{c_{EtOH} - \frac{c_{C2H4} c_{H2O}}{K_{III}}}{D} \quad (12)$$

$$r_5 = k'_5 \frac{c_{EtOH} - \frac{c_{C2H4O} c_{H2}}{K_V}}{D} \quad (13)$$

$$r_6 = k'_6 \frac{c_{DEE} c_{HCl} - \frac{c_{EtCl} c_{EtOH}}{K_{VI}}}{D} \tag{14}$$

$$D = (1 + K_{EtOH} c_{EtOH} + K_{HCl} c_{HCl})^2 \tag{15}$$

The kinetic data at different temperatures and HCl:EtOH ratios could not be fully described with the model represented by eqs. (10)-(15). Deviations for the ethylene and diethyl ether concentrations were observed at both high and low ratios of HCl:EtOH. In the case of a high HCl:EtOH ratio they were underestimated, while at a low HCl:EtOH ratio they were overestimated. This indicates that the HCl concentration influences the rate not only through adsorption on the catalyst surface, but also through modification of the catalyst surface characteristics, i.e. an increased acidity. A higher acidity of the alumina surface due to adsorbed HCl increases the rate of the ethanol dehydration reactions to ethylene and diethyl ether. To include this effect in the kinetic model and to improve the description of the ethylene and diethyl ether production at varying HCl:EtOH ratios an additional term (ε) was included in the rate expressions for these reactions. It expresses a catalytic effect of HCl and is used as multiplication factor in the rate expression of ethylene and diethyl ether formation. The value of ε was designed to approach the value one in the case that the HCl concentration approaches zero or if the parameter α approaches zero. This guarantees that the reactions do not stop when the HCl concentration becomes zero and allows the regression algorithm also to neglect the effect of HCl on the rate of ethylene and diethyl ether formation.

$$\varepsilon = (1 + c^*_{HCl})^{\alpha \frac{c^*_{HCl}}{c^*_{HCl} + c^*_{EtOH}}} \tag{16}$$

The model predictions and experimental data obtained at 280 °C for different HCl:EtOH ratios are displayed in Figure 26.

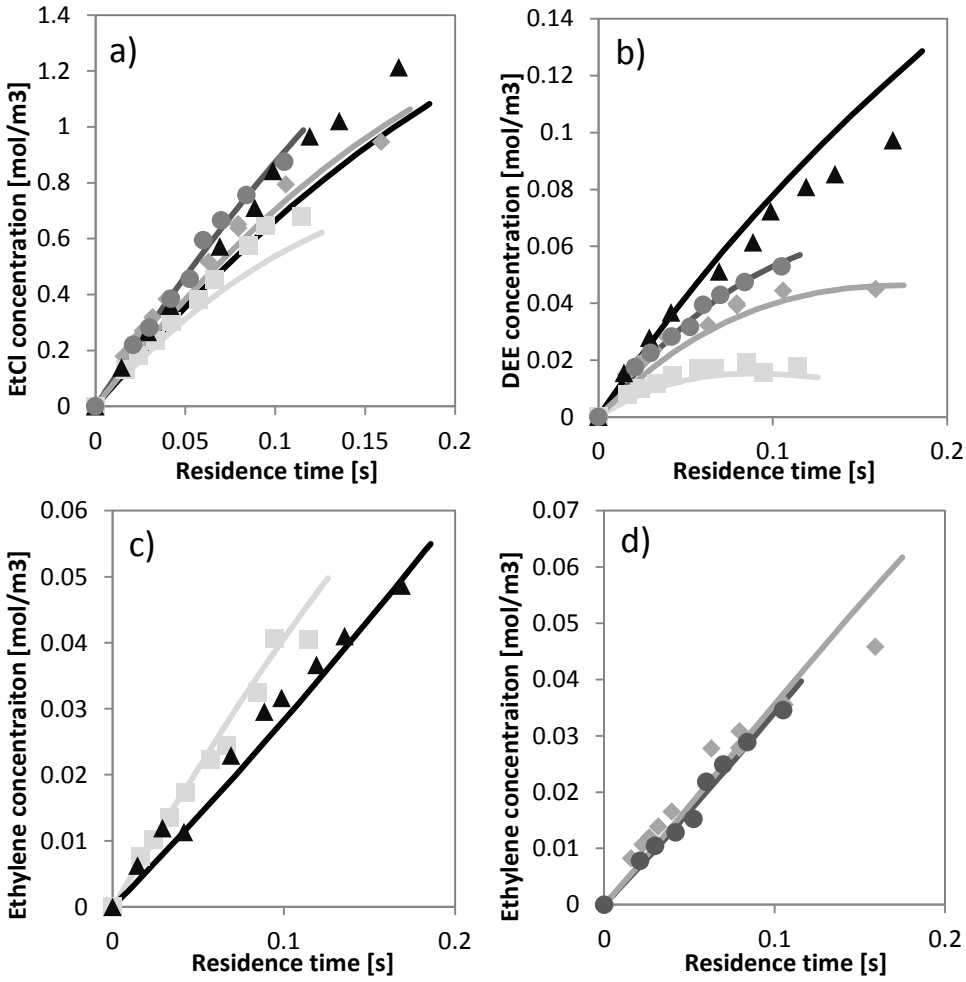

Figure 26: Model and experimental data for different HCL / EtOH concentrations [mol/m³] at 280 °C. a) ethyl chloride, b) diethyl ether, c) and d) ethylene, (■) 2.00: 0.98; (♦)1.91:1.88 ; (●)2.53:2.51; (▲)1.76:3.50.

The determined kinetic parameters of reactions (I)–(III), (V) and (VI) are summarized in Table 11. The activation energy and pre-exponential factor for the ethyl chloride and diethyl ether formation were determined with low errors (< 5%). The activation energy of ethyl chloride formation with 79 kJ/mol is in agreement with the results of Bukhanko et al. [33]. The parameters for the HCl adsorption and acetaldehyde formation are less precise with an error of 6.7 and 12 % respectively. The reason is the very low concentration of acetaldehyde and the high relative analytical error. Regressed adsorption constants are typically not well

Table 11: Kinetic parameters of reactions (I) –(III), (V) and (VI).

	A	Error [%]	E_A / [kJ/mol]	ΔH	Error [%]
Ethanol adsorption	0.7	<0.1	0.03		3.5
HCl adsorption	2.8	25	9.7		12
I (ethyl chloride)	$2.6*10^9$	3.3	78.9		4
II (diethyl ether)	$1.6*10^8$	0.3	83.4		0.3
III (ethylene)	$6.4*10^9$	2.4	102.1		2.4
V (acetaldehyde)	$2.0*10^4$	<0.1	25		<0.1
VI (EtCl from DEE)	$5.1*10^4$	6.7	51.6		6.3
α	6.7				

3.4 Reaction and separation (VI)

3.4.1 Production capacity of microreactor setup

When two serially coupled microreactors are used for the methyl chloride synthesis, equilibrium conversions and selectivities can be reached at temperature higher than 330 °C (Figure 27).

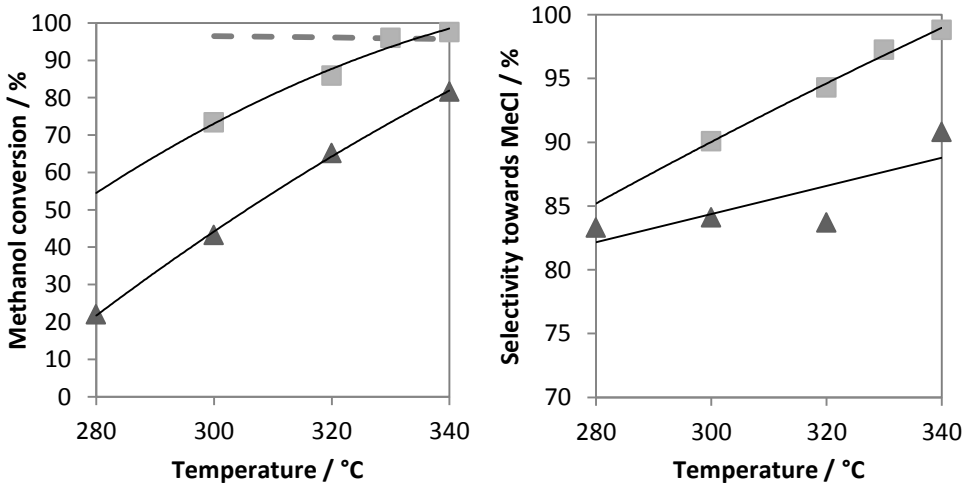

Figure 27: Influence of temperature on methanol conversion and methyl chloride selectivity in (▲) one and (■) two microreactors, (---) calculated thermodynamic equilibrium.

The catalyst-coated platelets were used at a temperature of 340 °C for 2750 min without observing a decrease of the performance. No corrosion of the microreactor housing was observed. However, a slight yellow color of the

catalyst layer after reaction for 2750 min indicates that corrosion takes place on the stainless steel surface below the catalyst coating. Neither the performance nor the catalyst layer stability was affected. Considerable corrosion of the lines was observed in places where the lines had a temperature below 100 °C and a corrosive mixture of water and HCl could condense. It is crucial that the equipment that is in contact with the reacted mixture is either kept well heated or is made of a corrosion resistant material such as Hastelloy, tantalum or glass.

The present setup made from two serially coupled GPMR microreactors by IMM produces ca. 0.8 kg of methyl chloride per year at the highest conversion and selectivity (97.5 %, 98.8 % at 340 °C). However, to suppress the corrosion problems the reaction mixture consisted of 82 % helium. If a concentrated reaction mixture can be used in a corrosion-resistant microreactor, the system would produce ca 5 kg of MeCl per year or 720 kg per year per g of catalyst. The production capacity of the two coupled microreactors is low. For actual production, the microreactors should be slightly larger, so that higher flow rates, i.e. production rates, can be sustained. The production capacity is increased by numbering up. Even though the production capacity of one microreactor is low, the catalyst efficiency is significantly enhanced. In a 15 μm thick catalyst layer, the effectiveness factor for methanol is 0.91 while in a 2 mm thick catalyst layer which corresponds to an industrial fixed bed the effectiveness factor drops to 0.03. The use of thin catalyst layers in microreactors thus considerably diminishes the equipment size compared to conventional fixed beds.

3.4.2 Separation of gaseous products

The product stream leaving the microreactor setup consists mainly of methyl chloride and water, with traces of dimethyl ether as well as unreacted methanol and hydrochloric acid. In industrial scale, methyl chloride is separated from dimethyl ether by extractive distillation. Prior to the distillation, water and unreacted HCl have to be removed [59]. Furthermore, methyl chloride can be purified by a series of scrubbers consisting of aqueous, caustic and sulfuric acid scrubbers. The first two scrubbers remove methanol, water and HCl from methyl chloride, while DME is trapped in the sulfuric acid scrubber [60].

In this work, the separation of methyl chloride and dimethyl ether from water, HCl and MeOH with a condenser was investigated. The use of a condenser avoids the production of large amounts of scrubber solutions and is less complex than extractive distillation. For a process that does not require high purity methyl chloride this separation method can be attractive.

Three condensers with different internal surfaces were compared. The smallest condenser was an Allihn condenser followed by Coil and Dimroth condensers.

The influence of the temperature and condenser design on the separation efficiency was studied. The composition of the gas phase was investigated with the microreactors giving an almost complete conversion, while the liquid phase analysis was performed at a lower conversion

(83.3%), since no considerable amounts of condensate could be obtained at higher conversion due to the low flow rate.

Using the smallest condenser, the methanol content detected in the gas phase decreased upon lowering the temperature of the cooling fluid from 0.6 wt% at +1 °C to 0.1 wt% at -10 °C. When a larger condenser was used or the temperature of the cooling fluid was further lowered to -15 °C, the methanol content of the gas phase could not be further reduced. The gas-phase composition prior to and after the different condensers is given in Table 12. Furthermore, the gas phase contains traces of HCl, which could not be determined quantitatively. However, the presence of HCl was confirmed by leading the gas over an amine solution: a white smoke consisting of ammonium chloride evolved.

Table 12: Composition of the gas stream obtained from Allihn, Coil and Dimroth condensers and the composition prior to the condenser.

Content / wt%	Prior	Allihn	Coil	Dimroth(-15 °C)
MeOH	2.50	0.13	0.08	0.14
MeCl	95.9	99.38	99.08	98.97
DME	1.60	0.49	0.84	0.90

The composition of the liquid phase collected from the condenser suggested though that most of the unreacted HCl remained in the condensate. The composition of the liquid phase for the Coil and the Dimroth condenser as well as the theoretical composition for complete condensation of water, methanol and HCl are given in Table 13. The composition of the gas phase leaving the condenser is specified in brackets. Both condensers gave a comparable separation of the liquid products. Only trace amounts of MeCl and DME were present in the condensate. The content of water increased compared to the theoretical composition (assuming complete condensation), while methanol is lower and the HCl content is close to the theoretical value. This shows that there is a considerable methanol slip and a minor HCl slip.

Table 13: Composition of condensate and gas phase [in brackets] obtained from Coil and Dimroth coolers at 83.3% conversion. 'Theoretical composition' means complete condensation of H_2O, HCl and MeOH.

Content / wt%	Theoretical composition	Coil	Dimroth(-15 °C)
H_2O	48.0	59	58
MeOH	18.2	8 [1.1]	13 [0.95]
HCl	33.8	33	29
MeCl+DME	-	0.08 [98.9]	0.04 [99.04]

4 Summary

A thorough study on methyl and ethyl chloride synthesis in a microreactor system has been carried out. This work included the screening of several potential catalysts and their in-depth characterization, the development of a stable and uniform catalyst coating, kinetic modeling and a study on of gaseous products separation by condensation.

Several catalysts were screened for the methyl chloride synthesis using a quartz-made tubular reactor: alumina, H-Beta and H-ZSM5 catalysts with varying Si/Al ratios, in neat form and modified with zinc chloride. In the case of $ZnCl_2$/alumina also the influence of the zinc loading was investigated. Modification with $ZnCl_2$ increased the activity and selectivity of all the catalysts studied due to the introduction of active and selective zinc-based Lewis acid sites. While the unmodified zeolite produces mainly hydrocarbons at low conversions, the zinc-modified zeolite is highly active and selective in the methyl chloride synthesis. In the case of zeolites, ion exchange takes place and the number of medium and strong Brønsted acid sites is diminished, while weak acid sites remain. In the case of alumina, zinc reacts with strong Lewis acid sites on the alumina surface leading to a gradual decrease of strong acid sites on alumina with an increasing zinc loading. Simultaneously an increase of weak zinc based Lewis acid sites which were highly active and selective in the methyl chloride synthesis was observed. A decrease of the specific surface area upon the introduction of zinc and with an increasing zinc loading suggests that bulk zinc species are formed as the number of sites for a molecular reaction of zinc with the support material decreases. In the case of zeolites, particles are formed on the catalyst surface, while in the case of alumina, an amorphous Zn^{2+} containing layer is formed on the alumina. As the atomic ratio Cl/Zn is significantly less than two, and it is gradually reduced upon the catalyst calcination, $ZnCl_2$ cannot be present as the bulk chemical phase. Thus, a mixed species Zn/O/Cl species is suggested. Zinc oxide was not detected, but $ZnCl_2$ and $ZnAl_2O_4$ could be defined as dominant bulk zinc species, based on electron diffraction measurements of the $ZnCl_2$/alumina catalysts.

A drawback of zeolite catalysts is that they are prone to deactivation especially for low Si/Al ratios. Due to the higher stability and selectivity, $ZnCl_2$/alumina with a loading between 5 and 10 wt% zinc was found to be the most suitable catalyst for the methyl chloride synthesis. Nevertheless, due to the very high activity and higher stability, H-ZSM5 based materials can be potential catalysts at lower temperatures. Despite the high stability in the tubular fixed bed reactor, the zinc-modified alumina and H-ZSM5 were not stable in the microreactor channels, due to a decrease in the selectivity with time-on-stream. For this reason, neat alumina was the catalyst of choice for the methyl and ethyl chloride synthesis in the microreactor.

A binder-free slurry coating method for the introduction of a stable catalyst coating was developed. The coating thickness can be adjusted and maintained constant by precisely controlling the amount of liquid placed on the platelet. The coating uniformity was improved by drying the platelets at

a lower temperature. The coating remained stable after application in the test reaction, as well as under nitrogen flow and ultrasound treatment. The stability of the coating is provided by thermal pretreatment of the platelets and ball-milling of the powder. Furthermore, the oxide layer formed in the thermal pretreatment protects the platelets from corrosion.

The performance of the microreactor was compared to the tubular fixed bed reactor by keeping the flow rate-to-catalyst mass ratio constant. It was shown that the performance of the microreactor was equivalent to the performance of the tubular reactor, suggesting that no reactor specific effects were present. The kinetics and thermodynamics of both methyl and ethyl chloride synthesis were investigated thoroughly.

Methyl chloride synthesis was performed in a single microreactor in the temperature range of 280-340 °C with a maximum conversion and selectivity of 83 % and 92 % respectively. Regarding thermodynamic equilibrium, it is recommended to perform the reactions at low temperatures to improve the conversion and selectivity. From a kinetic point of view, low temperatures as well are favorable for the selectivity, although activity will be too low. The developed kinetic model for methyl chloride synthesis takes into account both the methyl chloride and dimethyl ether formation. The influence of HCl and methanol adsorption on the catalyst surface was evaluated. Simulation of the coupled reaction and diffusion effects in porous catalyst layers revealed that mass transfer limitations prevail in catalyst pores, starting from a catalyst layer thickness of 50 µm at 300 °C. The simulations confirm that the kinetic results from the previous studies were influenced by mass transfer limitations.

Ethyl chloride synthesis was performed in a setup consisting of two serially coupled microreactors in the temperature range of 240 – 340 °C achieving an almost complete conversion at 340 °C. However, at this temperature the selectivity to ethyl chloride decreases significantly. The analysis of the thermodynamic equilibrium composition for the ethyl chloride synthesis predicted a high content of ethylene especially at high temperatures. To maximize the ethyl chloride production, the process should be carried out at low temperatures and with a well-controlled residence time. A detailed kinetic model was developed, describing the ethyl chloride, diethyl ether, ethylene and acetaldehyde formation and the effect of HCl on the rate of ethanol dehydration reactions.

The industrial feasibility of a microreactor system to produce methyl chloride was demonstrated. Using two serially coupled microreactors, the equilibrium conversion and selectivity were approached for the methyl chloride synthesis starting at 330 °C. The catalyst performance was tested for 2750 min at 340°C without any drop of the conversion and selectivity. The separation of the gaseous products from the liquid components using glassware condensers showed to be feasible and rather effective. The gas phase contained 99 wt% of methyl chloride, 0.5-0.9 wt% dimethyl ether and 0.1 wt% of methanol as well as traces of HCl. The condensate contained water and most of the unreacted HCl and methanol, while only traces, <0.01 wt%, of MeCl and DME could be detected in the condensate.

In conclusion, microreactors are feasible for the on-site hydrochlorination of methanol and ethanol using neat alumina as the catalyst. The main problem in the application of currently available microreactors is the corrosion due to the reactant HCl and the co-product,

water. Corrosion can lead to the destruction of the coating material as well as the reactor components and lines. However the design of the microreactor system used during this thesis can be optimized. A larger microreactor made of corrosion resistant material could be designed. The most important benefit of the use of a microreactor device is the increase of the space and catalyst effectiveness due to the suppression of internal diffusion limitations that are very severe in the hydrochlorination of methanol and ethanol in conventional fixed-bed reactors. Furthermore, the microreactor system showed to be an ideal tool for detailed kinetic investigations of the very fast reactions, minimizing the use and production of toxic chemicals and suppressing the diffusion limitations. The intrinsic reaction kinetics can be approached in microreactors even in in cases when it is a difficult or impossible task in conventional reactors.

5 Notations

A	frequency factor
c_i	concentration
D	denominator in rate equation
D_{ei}	effective diffusion coefficient
E_a	activation energy
K_i	equilibrium constant
k	rate constant
M	molar mass
N	stoichiometric number
P	total pressure
R_L	catalyst layer thickness
R	general gas constant
R^2	coefficient of determination;

$$R^2 = \frac{\sum (c_{i,\exp} - c_{i,\mathrm{mod}})^2}{\sum (\bar{c}_{i,\exp} - \bar{c}_{i,\mathrm{mod}})^2}$$

T	temperature
X	conversion
ε	term for HCl catalysis
η_i	effectiveness factor
ρ_B	catalyst bulk density
τ	residence time
φ	Thiele modulus

Chemical compounds

DEE	diethyl ether
DME	dimethyl ether
EtCl	ethyl chloride
EtOH	ethanol
MeCl	methyl chloride
MeOH	methanol

6 References

[1] K. Weissermehl, H.-J. Arpe, , 2003, Industrial organic chemistry, Wiley-VCH Verlag GmbH & Co. KGaA, Weinheim, 195 pp.

[2] ICIS Chemical Business Americas 2007, Methyl Chloride, 271, 50

[3] Source of pictures: Wikipedia.

[4] M. C. Miller, Ethyl Chloride, Kirk-Othmer Encyclopedia of Chemical Technology, John Wiley & Sons, New York, 2004.

[5] T. G. Majewicz, TJ. Podlas, Cellulose Ethers, Kirk-Othmer Encyclopedia of Chemical Technology, John Wiley & Sons, New York, 2001.

[6] H. Knözinger, R. Köhne, Catalytical dehydration of aliphatic alcohols on γ-Al2O3, J. Catal. 3 (1964), 559-560.

[7] H. Knözinger, R. Köhne, The dehydration of alcohols over alumina: I. The reaction scheme, J. Catal. 5 (1966), 264-270.

[8] A. P. Kagyrmanova, V. A. Chumachenko, V. N. Korotkikh, V. N. Kashkin, A. S. Noskov, Catalytic dehydration of bioethanol to ethylene: pilot-scale studies and process simulation, Chem. Eng. J. 176-177 (2011) 188-194.

[9] S. I. Ivanov, V. A. Makhlin, Catalytic interaction of methanol with hydrogen chloride on γ-Al2O3: Kinetics and mechanism of the reaction, Kinet. Catal.37 (1996), 812-818.

[10] I. I. Kurlyandskaya, S. B. Grinberg, T. F. Kudryavtseva, E. B. Svetlanov, R. M. Flid, R. V. Dzhagatspanyan, Investigation into hydrogen chloride and methanol catalyst interaction region, Russian Journal of Physical Chemistry 47 (1973), 189-93.

[11] E. B. Svetlanov, R. M. Flid, D.A. Gareeva, Catalytic interaction of hydrogen chloride and methanol. I. Kinetics of the vapor-phase, catalytic interaction of methanol and hydrogen chloride, Russian Journal of Physical Chemistry 40 (1966), 2302-2308

[12] T. M. Tovar, M. Stewart, S. L. Scott, Origin of the ZnCl2 Effect on CH3ReO3/γ-Al2O3 in Olefin Metathesis, Top. Catal. 55 (2012) 530-537.

[13] S. K. Pillai, S. Hamoudi, K. Belkacemi, Functionalized value-added products via metathesis of methyloleate over methyltrioxorhenium supported on ZnCl2-promoted mesoporous alumina. Fuel 110 (2013), 32–39.

[14] S. K. Pillai, S. Hamoudi, K. Belkacemi, Metathesis of methyloleate over methyltrioxorhenium supported on ZnCl2 promoted mesoporous alumina, Appl. Catal. A 455 (2013) 155–163.

[15] M. Conte, T. Davies, A. F. Carley, A. A. Herzing, C. J. Kiely ,G. J. Hutchings, Selective formation of chloroethane by the hydrochlorination of ethene using zinc catalysts, J. Catal. 252, (2007), 23–29.

[16]J. A. Biscardi, G. D. Meitzner, E. Iglesia, Structure and density of active Zn species in Zn/H-ZSM5 propane aromatization catalysts, J. Catal. 179 (1998), 192–202.

[17] L. Djakovitch, K. Koehler, Heck reactions catalyzed by oxide-supported palladium–structure–activity relationships, J. Am. Chem. Soc. 132, (2000), 5990.

[18] V. B. Kazansky, E. A. Pidko. Intensities of IR stretching bands as a criterion of polarization and initial chemical activation of adsorbed molecules in acid catalysis. Ethane adsorption and dehydrogenation by zinc ions in ZnZSM-5 zeolite. J. Phys. Chem. B 109(6), (2005) 2103-2108.

[19] R. Byggningsbacka, N. Kumar, L. E. Lindfors, Simultaneous dehydrogenation and isomerization of η-butane to isobutene over ZSM-22 and zinc-modified ZSM-5 zeolites. Catal. Let., 55(3-4), (1998), 173-176.

[20]V. B. Kazansky, L. M. Kustov, A. Y. Khodakov,. On the nature of active sites for dehydrogenation of saturated hydrocarbons in HZSM-5 zeolites modified by zinc and gallium oxides. Stud. Surf. Sci. Catal. 49, (1989), 1173-1182.

[21] V. R. Choudhary, K. Mantri,, Thermal activation of a clayzic catalyst useful for Friedel–Crafts reactions: HCl evolved with creation of active sites in different thermal treatments to ZnCl2/Mont-K10. Catal. Lett.81 (2002), 163-168.

[22] V.B. Kazansky, Localization of bivalent transition metal ions in high-silica zeolites with the very broad range of Si/Al ratios in the framework probed by low-temperature H2 adsorption, J. Catal. 216 (2003), 192–202

[23] S. Triwahyono, A. A. Jalil, R. R. Mukti, M. Musthofa, N. A. M. Razali, M. A. A. Aziz, Hydrogen spillover behavior of Zn/HZSM-5 showing catalytically active protonic acid sites in the isomerization of n-pentane, Appl. Catal. A 407 (2011), 91-99.

[24] G. M. Zhidomirov, A. V. Larin, D. N. Trubnikov, D. P. Vercauteren, Ion-exchanged binuclear clusters as active sites of selective oxidation over zeolites, J. Phys. Chem. C, 113 (2009), 8258-8265.

[25] N. H. N. Kamarudin, A. A. Jalil, S. Triwahyono, R. R. Mukti, M. A. A. Aziz, H. D. Setiabudi, H. Hamdan, Interaction of Zn with extraframework aluminum in HBEA zeolite and its role in enhancing n-pentane isomerization Appl. Catal. A 431-432 (2012), 104-112.

[26] V. B. Kazansky, V. Yu. Borovkov, A. I. Serikha, R.A. van Santen, B.G. Anderson, Nature of the sites of dissociative adsorption of dihydrogen and light paraffins in ZnHZSM-5 zeolite prepared by incipient wetness impregnation, Catal. Lett. 66 (2000) 39–47.

[27] V. I. Yakerson, T. V. Vasina, L. I. Lafer, V. P. Sytnyk, G. L. Dykh, A.V. Mokhov, O.V. Bragin, Kh. M. Minachev, The properties of zinc and gallium containing pentasils—The catalysts for the aromatization of lower alkanes, Catal. Lett.3 (1989) 339-346.

[28]J. Penzien, A. Abraham, J. A. van Bokhoven, A. Jentys, T. E. Mu1ller, C. Sievers J. A. Lercher, Generation and characterization of well-defined Zn2+ Lewis acid sites in ion exchanged zeolite BEA, J. Phys. Chem. B 108 (2004), 4116-4126.

[29] Svetlanov, E. B., Flid, R. M. Catalytic reaction of hydrochloric acid and methyl alcohol. II. Kinetics of reactions of methanol dehydration and dimethyl ether hydrochlorination on the catalysts of vapor-phase synthesis of MeCl. Zhurnal Fizicheskoi Khimii 40 (1966), 3055-3059.

[30] E. G. Schlosser, M. Rossberg, W. Lendle, Zur Kinetik der Methylchlorid-Bildung aus Methanol und Chlorwasserstoff an Aluminiumoxid, Chemie Ing. Techn. 42 (1970), 1215-1219.

[31] M. S. Thyagarajan, R. Kumar, N.R. Kuloor, Hydrochlorination of methanol to methylchloride in fixed catalyst beds, I&EC Proc. Des. Devel.5 (1966), 209-213.

[32] A. M. Becerra, A. E. Castro Luna, D. E. Ardissone, M. I. Ponzi, Kinetics of the catalytic hydrochlorination of methanol to methyl chloride, Ind. Eng. Chem. Res. 31 (1992), 1040-1045.

[33] N. Bukhanko, A. Samikannu, W. Larsson, A. Shchukarev, A. R. Leino, K. Kordas, J. Wärnå, J. P. Mikkola Continuous Gas-Phase Synthesis of 1-Ethyl Chloride from Ethyl Alcohol and Hydrochloric Acid Over Al2O3-Based Catalysts: The "Green" Route, ACS Sus. Chem. Eng. (2013), 1(8), 883-893,

[34] A. Erdőhelyi, J. Raskó, T. Kecskés, M. Tóth, M. Dömök, K. Baán, Hydrogen formation in ethanol reforming on supported noble metal catalysts, Catal. Tod. 116 (2006) 367–376.

[35] J. F. DeWilde, H. Chiang, D. A. Hickman, C. R. Ho, A. Bhan, Kinetics and Mechanism of Ethanol Dehydration on γ-Al2O3: The Critical Role of Dimer Inhibition, ACS Catalysis 3 (2013), 798-807.

[36] M. A. Christiansen, G. Mpourmpakis, D. Vlachos, Density Functional Theory-Computed Mechanisms of Ethylene and Diethyl Ether Formation from Ethanol on γ-Al2O3 (100), ACS Catalysis 3 (2013).

[37] V. Hessel, D. Kralisch, U. Krtschil, Sustainability through green processing–novel process windows intensify micro and milli process technologies, Energy Environ. Sci., 1 (2008), 467.

[38] G. Kolb, V. Hessel, Micro-structured reactors for gas phase reactions, Chemical Engineering Journal 98 (2004) 1.

[39] H. Pennemann, P. Watts, S. J. Haswell, V. Hessel, H. Löwe, Benchmarking of microreactor applications, Org. Proc. Res. Dev. 8 (2004), 422-439.

[40] A. Gavriilidis, P. Angeli, E. Cao, K. K. Yeong, Y. S.S. Wan, Technology and applications of microengineered reactors, Trans IChemE 80 (2002), 3-30.

[41] W. Ehrfeld, V. Hessel, H. Löwe, Microreactors: New Technologies for Modern Chemistry Wiley-VCH, Weinheim, 2004.

[42] V. Hessel, H. Löwe, F. Schönfeld, Micromixers—a review on passive and active mixing principles. Chem. Eng. Sci 60 (2005), 2479-2501.

[43] L. Kiwi-Minsker, A. Renken, Microstructured reactors for catalytic reactions, Catalysis Today, Volume 110 (2005), 2–14.

[44] J. Aubin, L. Prat, C. Xuereb, C. Gourdon, Effect of microchannel aspect ratio on residence time distributions and the axial dispersion coefficient, Chem. Eng. Proc. 48 (2009) 554–559.

[45] V. Meille, S. Pallier, P. Rodriguez, Reproducibility in the preparation of alumina slurries for washcoat application-Role of temperature and particle size distribution. Coll. Surf. A, 2009, 336, 104.

[46] C. A. Emeis, Determination of integrated molar extinction coefficients for infrared absorption bands of pyridine adsorbed on solid acid catalysts, J. Catal. 141 (1993), 347-354.

[47] L. Zhang, C. M. B. Holt, E. J. Luber, B. C. Olsen, H. Wang, M. Danaie, X. Cui, X. Tan, V. Lui, W. P. Kalisvaart, D. Mitlin, High rate electrochemical capacitors from three-dimensional arrays of vanadium nitride functionalized carbon nanotubes, J. Phys. Chem. C 115 (2011) 24381-24393.

[48] C. D. Chang, Methanol Conversion to Light Olefins, Catal.Rev.Sci. Eng. 26 (1984), 323–345.

[49] C.E. Taylor, Conversion of substituted methanes over ZSM-catalysts, Stud. Surf.Sci. Catal.130 (2000), 3633.

[50]J. W. Park, G. Seo, IR study on methanol-to-olefin reaction over zeolites with different pore structures and acidities Appl.Catal. A 356.2 (2009), 180-188.

[51] S. Arndt, B. Uysal, A. Berthold, T. Otrebma1, Y. Aksu, M. Driess, R. Schomäcker, Supported ZnO catalysts for the conversion of alkanes: About the metamorphosis of a heterogeneous catalyst, J. Natur. Gas Chem. 21 (2012) 581–594.

[52] N. S. Gill, R. H. Nuttall, D. E. Scaife, D. A. J. Sharp, The infra-red spectra of pyridine complexes and pyridinium salts, Inorg. Nucl. Chem. (1961) 18, 79-87.

[53] M. Digne, P. Sautet, P. Raybaud, P. Euzen, H. Toulhoat, Hydroxyl groups on γ-alumina surfaces: A DFT study, J. Catal. 211 (2002) 1-5.

[54] A. A. Tsyganenko, V.N. Filimonov, Infrared spectra of surface hydroxyl groups and crystalline structure of oxides , J. Mol. Struct. 19 (1973) 579-589.

[55] R. Zapf, G. Kolb, H. Pennemann, V. Hessel, Basic study of adhesion of several alumina-based washcoats deposited on stainless steel microchannels. Chem. Eng. Technol., 2006, 29, 1509.

[56]A. R. McInroy, D.T. Lundie, J. M. Winfield, C. C. Dudman, P. Jones, D. Lennon, The Application of Diffuse Reflectance Infrared Spectroscopy and Temperature-Programmed Desorption to Investigate the Interaction of Methanol on η-Alumina. Langmuir 21 (2005) 11092–11098.

[57] A. Kytökivi, M. Lindblad, A. Root, IR and 1H NMR studies on the adsorption of gaseous hydrogen chloride on γ-alumina. J. Chem. Soc. Faraday Trans. 91 (1995), 941-948.

[58] E.-Y. Lee, Y.-K. Park, O.-S. Joo, K.-D. Jung, Methanol Dehydration to produce Dimethyl Ether over γ -Al2O3. React. Kinet. Catal. Lett. 89 (2006), 115-121.

[59] P. Roth, E. Leistner, H. Haverkamp, W. Wendel, M. Kleiber, Process for the separation of dimethyl ether and chloromethane in mixtures, 1999, U.S. Patent No. 5,882,485. Washington, DC: U.S. Patent and Trademark Office.

[60] E. A. Thronson, Purification of methyl chloride, 1947, U.S. Patent No. 2,421,441. Washington, DC: U.S. Patent and Trademark Office.

ISBN 978-952-12-3101-8
Painosalama Oy - Åbo/Turku Finland